ELSEVIER

Tectonophysics 283 (1997) 1–33

TECTONOPHYSICS

Structure and deformation of north and central Malaita, Solomon Islands: tectonic implications for the Ontong Java Plateau–Solomon arc collision, and for the fate of oceanic plateaus

M.G. Petterson [a,1], C.R. Neal [b,*], J.J. Mahoney [c], L.W. Kroenke [c], A.D. Saunders [d], T.L. Babbs [d], R.A. Duncan [e], D. Tolia [a], B. McGrail [a]

[a] *Water and Mineral Resources Division, P.O. Box G37, Honiara, Solomon Islands*
[b] *Department of Civil Engineering and Geological Sciences, University of Notre Dame, Notre Dame, IN 46556, USA*
[c] *SOEST, University of Hawaii, 2525 Correa Road, Honolulu, HI 96822, USA*
[d] *Department of Geology, University of Leicester, University Road, Leicester, LE1 7RH, UK*
[e] *College of Oceanography, Oregon State University, Corvallis, OR 97331, USA*

Received 4 December 1996; accepted 18 August 1997

Abstract

The island of Malaita, Solomon Islands, represents the obducted southern margin of the Ontong Java Plateau (OJP). The basement of Malaita formed during the first and possibly largest plateau-building magmatic event at ~122 ± 3 Ma. It subsequently drifted passively northwards amassing a 1–2 km thickness of pelagic sediment overburden. A major change in OJP tectonics occurred during the Eocene, possibly initiated by the OJP passing over the Samoan or Raratongan hotspot. Extension facilitated increased sedimentation and basin formation (e.g., the Faufaumela basin) and provided readily available deep-crustal pathways for alkali basalt and subsequent Oligocene alnöite magmas, with related hydrothermal activity producing limited Ag + Pb mineralisation. Eocene to Mid-Miocene sediments record the input of arc-derived turbiditic volcaniclastic sediment indicating the relative closeness of the OJP to the Solomon arc. The initial collision of the OJP and Solomon arc at 25–20 Ma was of a 'soft docking' variety and did not result in major compressive deformation on Malaita. South-directed subduction of the Pacific Plate briefly ceased at this time but resumed intermittently on a local scale from ~15 Ma. Subduction of the Australian Plate beneath the Solomon arc commenced at ~8–7 Ma. Increased coupling between the Solomon arc and the OJP led to the gradual emergence of the OJP at 6–5 through to 4 Ma. The most intense period of compressive to transpressive deformation recorded on Malaita is stratigraphically bracketed at between 4 and 2 Ma, resulting in estimated crustal shortening of between 24 and 46%, and the inclusion of between 1 and 4 km of basement OJP basalts within the larger anticlines. Basement and cover sequences are deformed together in a coherent geometry and there are no major decollement surfaces; the large asymmetrical fold structures of Malaita are likely to be the tip regions of blind thrusts with detachment surfaces between 1 and 4 km beneath the cover sequence. Mid-Pliocene deformation records the detachment of the upper parts of the OJP, with initial material movement direction towards the northeast and later obduction of an upper allochthonous block of the OJP southwestwards over the Solomon arc. A model is presented whereby an upper 5–10-km-thick flake of the OJP is obducted over the Solomon arc to form the Malaita

* Corresponding author. Fax: +1-219-631-9236; e-mail: Neal.1@nd.edu
[1] Present address: British Geological Survey, West Mains Road, Edinburgh EH9 3LA, UK.

PII S0040-1951(97)00206-0

anticlinorium, whilst deeper levels are presently being subducted. The important implication is that even very large and thick oceanic plateaus may not survive subduction completely intact.

Keywords: oceanic plateaus; obduction; subduction; island arc; stratigraphy; Solomon Islands

1. Introduction

The ultimate fate of oceanic plateaus is important for understanding the evolution of oceanic large igneous provinces (LIPs) and is also a subject which is of fundamental importance to models of continental crustal accretion and growth from the Archaean to the present day. The key question is how permanent are oceanic plateaus? Are they ephemeral structures which are subducted and recycled back into the mantle along with other, more 'normal' parts of the ocean floor, or do some survive subduction and become permanent, obducted components of continental crust? Approximately 3% of the present-day ocean floor is composed of plume-related thickened basaltic crust, of which oceanic plateaus are the largest and most dramatic examples. If these structures survive subduction they will be a major factor in the rate of continental crustal accretion over geological time, and would rival arc accretion in terms of volume as a continental crust-forming phenomenon (Kroenke, 1972; Ben-Avraham et al., 1981; Nur and Ben-Avraham, 1982). Cloos (1993) calculated that basalt-dominated oceanic plateau crust must exceed ~17 km thickness to survive subduction, and must exceed ~30 km before causing significant deformation, or 'collisional orogenesis' during subduction. Several workers claim to have identified obducted oceanic plateau terranes on continental crust: the best known examples are the Wrangellia terrane of Alaska and British Columbia (e.g., Richards et al., 1991), and Gorgona Island, Colombia (e.g., Duncan and Hargreaves, 1984; Storey et al., 1991). However, examples of indisputable obducted oceanic plateau material within present-day continental crust are relatively uncommon; this could suggest that oceanic plateaus have a low preservation potential, are only obducted under exceptional circumstances, or that we are only now realising the criteria by which obducted oceanic plateau terranes can be recognised (e.g., Mahoney, 1987).

Fortunately, the Ontong Java Plateau (OJP) in the SW Pacific affords the opportunity of studying the tectonic effects of an oceanic plateau at a subduction zone. Residing at the boundary between the Australian and Pacific plates, it has caused the reversal of subduction polarity (e.g., Coleman and Kroenke, 1981). Along the southern border of the OJP, the Solomon Islands mark the boundary between the two plates and the basement of Malaita, Ulawa, Ramos, and the northern portion of Santa Isabel is composed of emergent OJP (e.g., Mahoney et al., 1993a,b; Saunders et al., 1993; Petterson, 1995; Tejada et al., 1996; Neal et al., 1997). This paper presents results from a major geological survey of the island of Malaita, Solomon Islands, undertaken by the Solomon Islands Geological Survey between 1990 and 1994, which has resulted in a series of geological maps, and two geological memoirs (Petterson, 1995; Mahoa and Petterson, 1995). Concomitant with the geological mapping were major sampling trips by several of the present authors which have yielded geochemical, geochronological, and isotopic data on the basaltic basement of Malaita. Geological and structural mapping of Malaita provides unique insights into the collisional and pre-collisional tectonic history of the OJP as it drifted towards, and finally collided with, the Solomon arc. Structural data from Malaita are coupled with seismic swath mapping and geological data from the region around Malaita to formulate a model for the collision of the OJP and the Solomon arc which is proposed below.

2. Regional tectonic and geological setting

The greater part of the island archipelago nation, Solomon Islands, forms a linear double chain of islands, oriented NW–SE between latitudes 5–10° south, and longitudes 156–163° east, in the southwest Pacific (Figs. 1 and 2). Solomon Islands are a component of the Greater Melanesian Arc System which marks the collisional zone between the Aus-

tralian and the Pacific plates which includes (from northwest to southeast) the islands of New Britain and Bougainville in Papua New Guinea, Solomon Islands, and Vanuatu (formerly known as New Hebrides). At the present time the Australian Plate is subducting beneath the Pacific Plate, and has been doing so for approximately the past 12 m.y. (e.g., Yan and Kroenke, 1993).

Solomon Islands are the subaerial tip of an upstanding topographic block (e.g., Petterson, 1995), the Solomon Islands block, which is bounded by two trench systems, one located to the northeast (the Vitiaz trench system), and one located to the southwest (the South Solomon trench system) (Figs. 1 and 2). The Solomon Islands block comprises a series of topographic highs which form the islands and other shallow-submarine topographic structures, as well as a series of deeper intra-block sedimentary basins with sea depths of $\leq$1 km. The Vitiaz trench system extends ~2500–3000 km in a NW–SE to E–W direction from the Kilinailau trench, north of the Taba-Feni Islands (Papua New Guinea) through the North Solomon, Ulawa, and Cape Johnson trenches, to the Vitiaz trench itself (Figs. 1 and 2). The Vitiaz trench system varies in depth between approximately 3000 m and 6000 m. The South Solomon trench system (SSTS) is divisible into three distinct parts which are (from northwest to southeast): (1) the New Britain trench (maximum depths of between 5000 m and 9000 m); (2) the area of trench shoaling between Bougainville and Guadalcanal (maximum water depths of between 2500 and 5000 m); and (3) the San Cristobal trench (with maximum depths of between 5000 m and 7500 m).

The great bulk of the OJP is located north of the Vitiaz trench, much of it standing at a general elevation of ~2 km above surrounding the ocean floor (e.g., Kroenke, 1972). At the time of writing ^{40}Ar–^{39}Ar ages of basalt samples from the islands of Malaita and Santa Isabel and Deep Sea Drilling Project (DSDP) and Ocean Drilling Project (ODP) boreholes into the OJP suggest a bimodal distribution of ages with one data population clustering around 122 $\pm$ 3 Ma and a second population clustering around 90 $\pm$ 4 Ma (Mahoney et al., 1993a,b; Tejada et al., 1996). These data have been interpreted by Bercovici and Mahoney (1994) as indicating that the plateau may have formed during two discrete magmatic events related to mantle plume dynamics. However, it is also possible that the apparent bimodality of the age data reflects the sparse sampling of the Alaska-sized OJP, and it is still a possibility that the plateau was formed over a more protracted period (e.g., Ito and Clift, 1996). After plateau formation, subsequent plate movements juxtaposed the OJP alongside the Solomon block at ~25–20 Ma (e.g., Coleman and Kroenke, 1981; Kroenke, 1984; Yan and Kroenke, 1993).

Solomon Islands are not a simple arc system but represent a collage of crustal terranes with discrete and complex geological histories. This fact was first recognised by Coleman (1965, 1966, 1970) and Hackman (1973), who divided this region into three distinct geological provinces.

(1) The Pacific Province to the east appears to be an uplifted and largely unmetamorphosed portion of the OJP, and forms the basement of Malaita, Ramos, Ulawa, and north of the Kaipito–Korighole fault system on Santa Isabel (e.g., Hawkins and Barron, 1991; Petterson, 1995; Tejada et al., 1996).

(2) The Central Province is adjacent to the Pacific Province in the southwest and contains variably metamorphosed Cretaceous and early Tertiary seafloor and remnants of the northeast-facing arc sequence that grew during the early to middle Tertiary above the then southwest-plunging Pacific Plate (prior to the arrival of the OJP from the east).

(3) The Volcanic Province, which extends along the southwestern flank of the Central Province, is an island arc sequence composed of volcanic and intrusive rocks and active volcanoes; the age of this province appears to be <4 Ma (e.g., Petterson, 1995).

However, subsequent mapping and geochemical investigations have shown that this 'province model' is an oversimplification of the tectonic processes which have affected this region. An alternative model has been proposed by Petterson (1995) and Petterson et al. (1997) which incorporates the findings of recent work, and subdivides the Solomons into five distinct terranes on the basis of basement age and composition and subsequent arc development (or lack thereof).

The oldest basement of many of the Solomon Islands was formed either at a normal ocean ridge and is composed of normal or N-type MORB, or

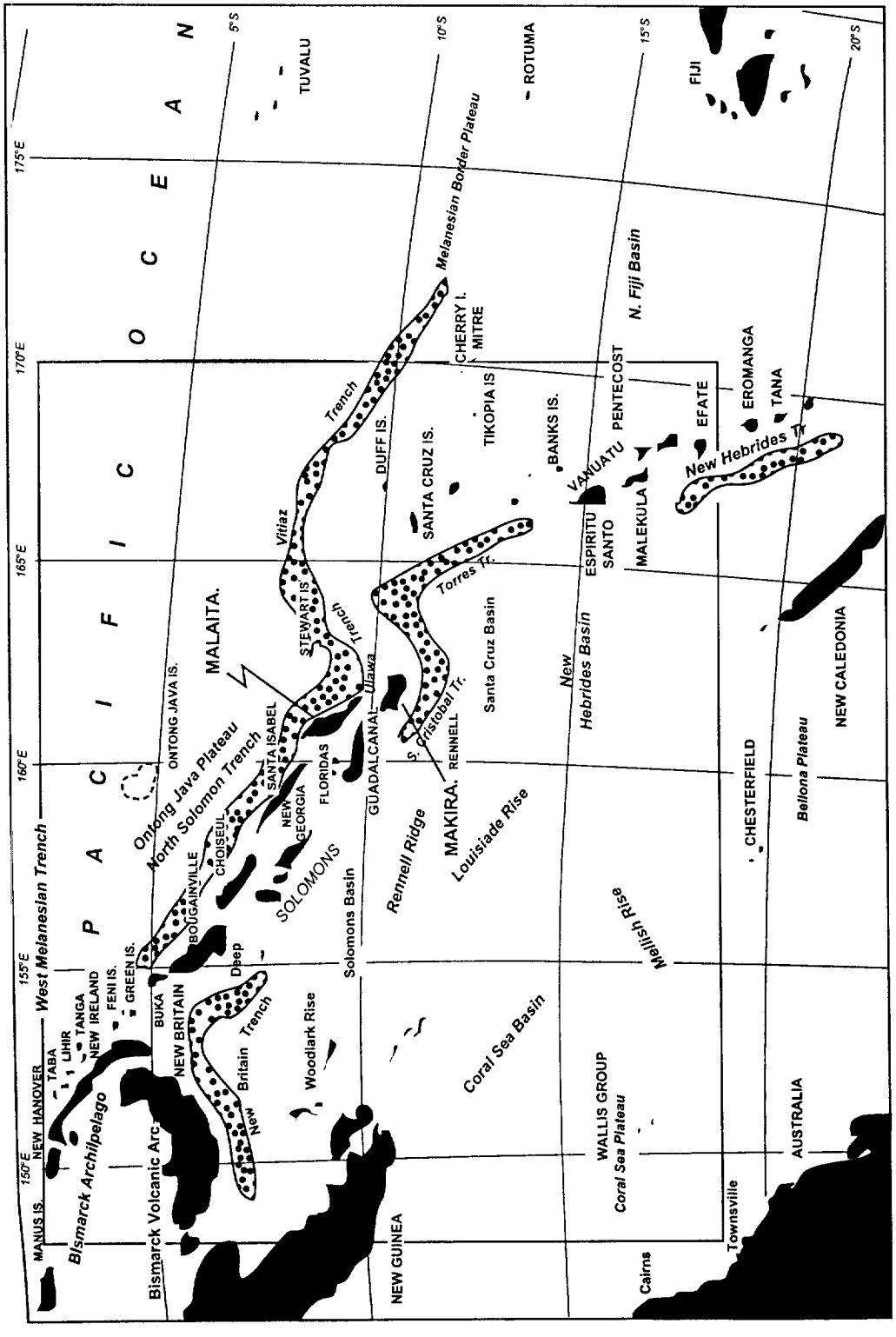

Fig. 1. Regional setting of Solomon Islands within the SW Pacific. The surface expression of the Solomon block is a double chain of islands bounded by the Vitiaz and New Britain–San Cristobal trench systems. The box indicates the region depicted in Fig. 2.

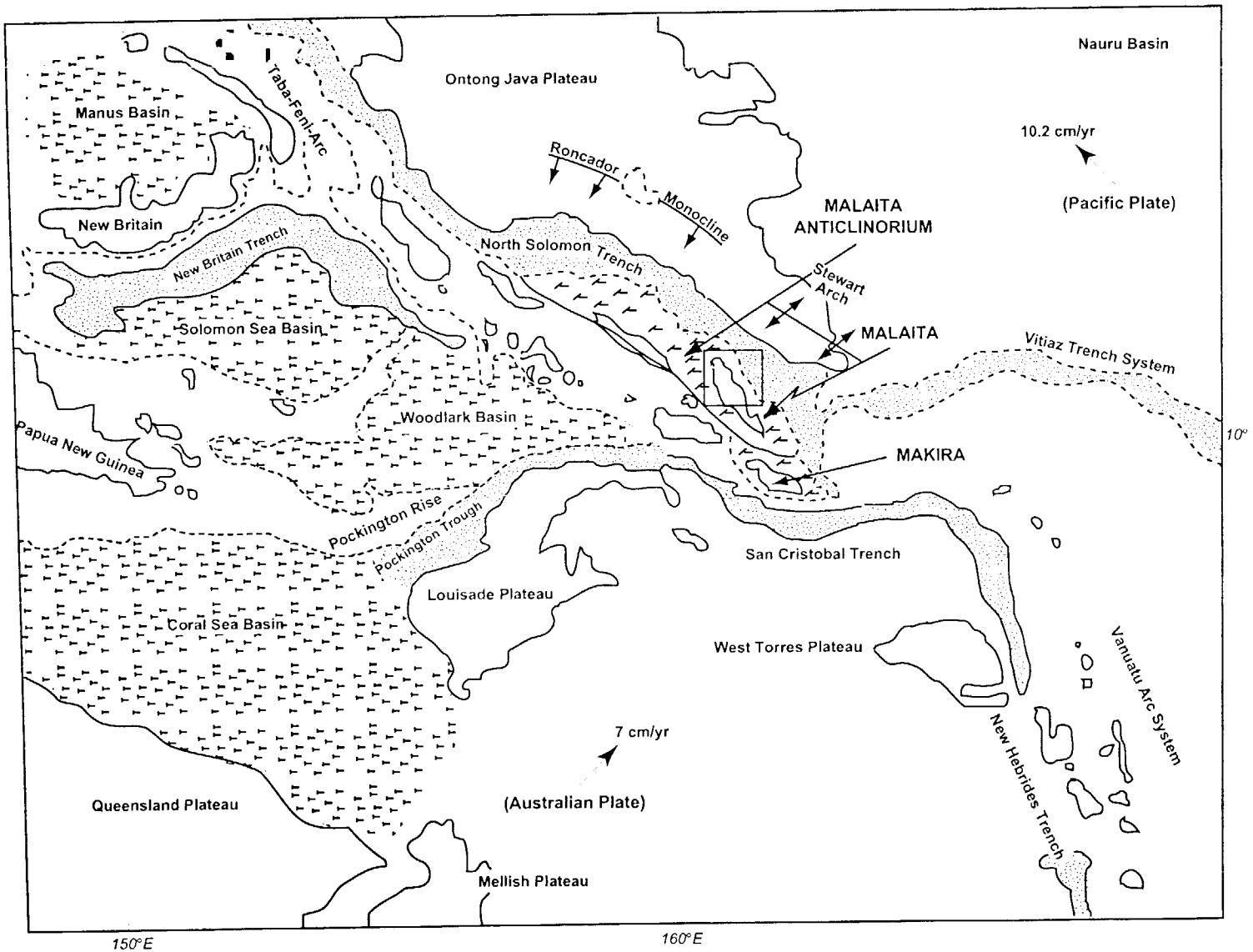

Fig. 2. Basins, blocks and trenches within the Solomon Islands region (the area defined by the box in Fig. 1). Note how the North Solomon trench system physically separates autochthonous OJP from detached OJP (the Malaita anticlinorium). The box indicates the area depicted in Fig. 5.

was formed as part of the OJP magmatic events and has a plume-related basalt composition. Subsequently, there were two stages of arc development which transformed the bulk of the Solomon block from being basalt-dominated, to a basalt plus andesite, arc-like, crustal composition. 'Stage-1' arc development (Table 1) occurred during the Eocene–Early Miocene (Kroenke, 1984) and resulted from southwestwards-directed subduction of the Pacific Plate beneath the Australian Plate along the Vitiaz/North Solomon trench. Arc-related volcanic and volcaniclastic rocks of this age occur on the islands of Guadalcanal, Choiseul, the Floridas, south Santa Isabel, and the Shortland Islands (Neef and Plimer, 1979; Hackman, 1980; Turner and Ridgeway, 1982; Kroenke, 1984; Pound, 1986; Coulson and Vedder, 1986; Ridgeway and Coulson, 1987). Subduction ceased along the Vitiaz trench during the Mid-Miocene, possibly because of the entry of the OJP into the Vitiaz trench (e.g., Coleman and Kroenke, 1981; Table 1). Northeast-directed subduction commenced during the Late Miocene along the South Solomon trench and resulted in Upper Miocene–present-day 'Stage-2' arc accretion on the islands of Choiseul, the New Georgia Group, the Russell Islands, Savo, Guadalcanal, Makira (San Cristobal), the Shortlands, and possibly the Floridas (Hackman, 1980; Chivas, 1981; Dunkley, 1983, 1986; Kroenke, 1984; Pound, 1986; Coulson and Vedder, 1986; Ridgeway and Coulson, 1987; Petterson, 1995; Petterson et al., 1997).

The thick OJP basalt sequences of several of the major islands (Malaita, northern Santa Isabel, Ramos, Ulawa) within the Solomon Islands have equivalent pelagic limestone ± chert cover sequences to those encountered in the ODP and DSDP boreholes on the OJP (Kroenke, 1972; Hughes and Turner, 1977; Berger et al., 1992; Kroenke et al., 1993; Petterson, 1995). Kroenke (1972) demonstrated a remarkable degree of continuity in seismic reflection stratigraphy between the 'Malaita anticlinorium' (Fig. 2) and the OJP itself. The Malaita anticlinorium is a region within the Solomon block which has undergone significant deformation resulting in regional folding and thrusting; these structures have been mapped onland (e.g., Hughes and Turner, 1976; Danitofea, 1981; Hawkins and Barron, 1991; Petterson, 1995), and seismically imaged offshore (e.g., Kroenke, 1972; Kroenke et al., 1986; Sopacmaps, 1994). The Malaita anticlinorium is interpreted by many workers (e.g., Kroenke, 1984) as the obducted part of the OJP. The island of Malaita is where the thickest sequence of OJP crust is exposed subaerially and where the deformation which resulted in the Malaita anticlinorium can be most clearly studied.

2.1. Age constraints on tectonic models relating to Solomon Islands

Tectonic models relating to the Solomon Islands region described above are a summary interpretation based on models published in the literature and recent work undertaken by the authors. As such, Section 2 presents a consensus view. However, we feel that we must emphasise that these models are based partly on sparse, and often imprecise age data, and questionable assumptions concerning the relationship between subduction and magmatism in arc systems. For example, prior to the recent investigations of the present authors, only ~12 age determinations have been published from the whole of the Solomons chain; several of these have large experimental errors and were determined by whole-rock K/Ar techniques (e.g., Richards et al., 1966; Snelling et al., 1970; Hackman, 1980; Dunkley, 1983). There are some additional constraints provided by palaeontological and stratigraphical studies, but this still leaves very large gaps in our geochronological understanding of the Solomon Islands, although present Ar/Ar age-dating studies are beginning to fill in these gaps. Another problem with present-day tectonic models relates to the timing of the Stage-1 and Stage-2 arcs; how do we actually define when one arc system ends and another one begins? At present, this interpretation is based upon an apparent cessation in magmatism in the Mid-Miocene. Future geochronological studies may show that, in reality, there may be no such cessation, and even if there were it does not necessarily mean that one subduction system has ended and another one taken over, but may merely reflect a temporary halt in magma production within a single subduction system.

3. Outline of geology of Malaita

3.1. Previous geological investigations

The first reconnaissance geological map of Malaita (Rickwood, 1957) only covered the northern portion of the island. Using photogeological evidence as well as field traverses, Allum (1967) produced a geological map which covered the entire island. Prior to this work, the most comprehensive studies of Malaita geology were conducted by Hughes and Turner (1976, 1977), who concentrated on south Malaita, with Hine (1991) and Barron (1993) concentrating on northernmost Malaita. Furthermore, the cover sediments were reported to range in age from Cretaceous to Tertiary (e.g., McTavish, 1966; Coleman, 1966; Van Deventer and Postuma, 1973) and the structure in these sediments was studied by Hackman (1968). Several petrographic, geochemical, and petrogenetic studies have been made of the Oligocene alnöites of Malaita (e.g., Rickwood, 1957; Allen and Deans, 1965a,b,c, 1968; Nixon and Coleman, 1978; Neal, 1985, 1988; Nixon and Neal, 1987; Neal and Davidson, 1989). Paradoxically, these unusual and volumetrically miniscule rocks were the most understood rocks in Malaita before the present study.

3.2. Stratigraphic summary

The geology of Malaita reflects its unique position as an obducted part of the Alaska-sized OJP. As such, the geology comprises a mono-lithological Cretaceous basalt basement sequence up to 4 km thick, here termed the Malaita Volcanic Group (MVG), conformably overlain by a Cretaceous–Pliocene pelagic sedimentary cover sequence (Figs. 3 and 4). Estimated total thicknesses of the Malaitan cover sequence are 1–3 km, which is somewhat thicker than sediment thicknesses measured in DSDP/ODP cores from the submerged OJP (<1.3 km; e.g., Kroenke et al., 1991); this may suggest that the Malaitan sequence has experienced local tectonic thickening. Cretaceous to Pliocene pelagic sedimentation was punctuated by alkaline basalt volcanism during the Eocene at ~44 Ma (Tejada et al., 1996), and ultramafic (alnöite) intrusive activity during the Oligocene at ~34 Ma (Davis, 1977). Basement and cover sequences were both deformed by an intense but short compressive to transpressive deformation event during the mid-Pliocene. A number of localised Upper Pliocene–Pleistocene, shallow-marine to subaerial, predominantly clastic formations overlie a mid-Pliocene unconformity surface (Petterson, 1995).

The MVG yield ^{40}Ar–^{39}Ar plateau ages of 122 ± 3 Ma (Aptian, Lower Cretaceous) (R.A. Duncan, unpubl. data; Tejada et al., 1996). The MVG are a monotonous sequence of pillowed and non-pillowed tholeiitic basalt lavas and sills composed of a predominant clinopyroxene–plagioclase tholeiitic mineralogy with minor glass + opaques and rare corroded olivine phenocrysts. Lava/sill thicknesses vary between 80 cm and 50–60 m with modal thicknesses of between 4 and 12 m; this variation in lava thicknesses possibly reflects inputs from both proximal and distal sources, and/or variations in the ruggedness and topography of the seafloor. The plateau morphology of the MVG is reflected in the presence of trap-like topographic features exposed in numerous river sections. There is remarkably little non-basaltic sediment present between sheets (most inter-sheet contacts observed are basalt–basalt contacts) indicating very high effusion rates. When present, intra-sheet sediment usually comprises laminated pelagic chert with only rare limestone, millimetres to a few centimetres thick, reflecting a deep-water emplacement of the basalts equivalent to, or deeper than the carbonate compensation depth (CCD) at that time; the predominance of chert over limestone as inter-sheet material implies that the bulk of the eruptions occurred below the CCD (see below). Gabbroic intrusions, dolerite dykes, and an unusual spherulitic dolerite facies are present locally. The geochemical composition of the MVG is intermediate between 'N'- and 'E'-type MORB, typical of plateau basalts (e.g., Mahoney, 1987; Neal et al., 1997); geochemical and isotopic data lie within geochemical fields defined by OJP samples from the ODP and DSDP boreholes, indicating essentially identical compositions (Fig. 5). The MVG formed as part of the OJP during the first major magmatic event related to the OJP plume as no 90 Ma lavas have been found on Malaita.

Immediately overlying the MVG is the 100–270-m-thick, Lower to mid-Cretaceous Kwaraae Mud-

Table 1
Tectonic chronological summary of OJP, Malaita, and Malaita anticlinorium

Tectonic event	Associated structures	Volcanism/sedimentation	Timing	References
Formation of OJP.	Extensional structures related to oceanic plateau formation.	Massive ?fissure or ?rift-centred, plume-related, basaltic magmatism.	122 Ma and ~90 Ma	Mahoney et al. (1993a), Tejada et al. (1996)
Passive movement of OJP southwards, punctuated by ?plume-related magmatism.	Extensional structures related to 90 Ma plateau-building event. Local (e.g. Faufaumela) basin formation from the Eocene.	Deep-sea pelagic sedimentation punctuated by 90 Ma plateau-building basalt, 44 Ma alkaline basalt, and 34 Ma alnöite magmatism.	From initial plateau formation to Miocene.	Hughes and Turner (1976, 1977), Petterson (1995)
Stage-1 Solomon arc. South-directed subduction at Vitiaz trench.	Formation of Vitiaz trench and Solomon arc–block.	Arc-related magmatism and sedimentation on numerous Solomon islands.	Paleocene/Eocene–Lower Miocene.	Kroenke (1984), Coulson and Vedder (1986)
First contact: OJP and Solomon arc–block. Cessation of Stage-1 Solomon arc; temporary cessation of S-directed subduction at Vitiaz trench.	Arching of OJP on approach to Vitiaz trench with associated extensional faults. Thrust faulting in trench area.	Final stage of Stage-1 Solomon arc magmatism. Poha diorite age of 24 ± 0.4 Ma. Continued deep-sea sedimentation on Malaita.	25–22 Ma	Kroenke (1972, 1984), Chivas (1981), Yan and Kroenke (1993)
'Soft docking' collisional stage between OJP and Solomon block.	Possible commencement of thrust and strike-slip deformation within collisional zone of Malaita anticlinorium.	Continued deep-sea sedimentation in Malaita area.	25–22/8–7 Ma	

Table 1 (continued)

Tectonic event	Associated structures	Volcanism/sedimentation	Timing	References
Intermittent S-directed subduction of OJP at Vitiaz trench.		First phase of Choiseul volcanism ca. Mid-Miocene. Second phase of Choiseul volcanism together with Vitiaz volcanism east of Ulawa, from the Pliocene.	First volcanic stage began ?~15 Ma. Main volcanic stage from ~5 Ma.	Ridgeway and Coulson (1987), Sopacmaps (1994), L.W. Kroenke (unpubl. data).
Commencement of Stage-2 Solomon arc; N-directed subduction at South Solomon trench.	Uplift of South Solomon block. Volcanism within pull-apart grabens resulting from oblique collision. Intermittent compression, folding, and/or tilting.	Stage-2 arc volcanism and sedimentation on Makira, Guadalcanal, Savo, Russells, New Georgia Group. Earliest determined radiometric age for Gallego volcanics of Guadalcanal: 6.4 + 1.9 Ma.	~12 Ma in Fiji area, ?~7 Ma in Guadal. Makira area	Hackman (1980), Dunkley (1986), Yan and Kroenke (1993)
Emergence of Malaita to shallow-marine depths.	Formation of isolated marine basins (e.g. Suafa Fm. deposits of Malaita).	Change from deep-sea to shallow-marine sedimentary facies on Malaita.	?6/5 -4 Ma	Hine (1991)
'Hard docking stage'. Major (~30%) shortening of Malaita. NE- SW compression and NW-SE strike-slip on Malaita.	N-verging asymmetrical folds and thrust faults. Some of these are re-activated normal faults on Malaita.	?Possible shedding of sediment from frontal thrust ramps within Malaita anticlinorium.	4–2 Ma	Kroenke (1972, 1984)
Obduction of upper ?5–10 km of S-OJP crust towards the southwest across the N Solomon trench, and over Solomon arc–block. Deeper parts of OJP subducted.	SW verging backthrusts on Malaita. Submarine ridges within Malaita anticlinorium imaged by sopacmaps interpreted as SW-directed thrusts.	Deposition of localised shallow-marine to fluvial sediments on Malaita. Frontal thrust ramparts shedding sediment into foreland marine basins.	2–0 Ma	Sopacmaps (1994), Kroenke (1995)

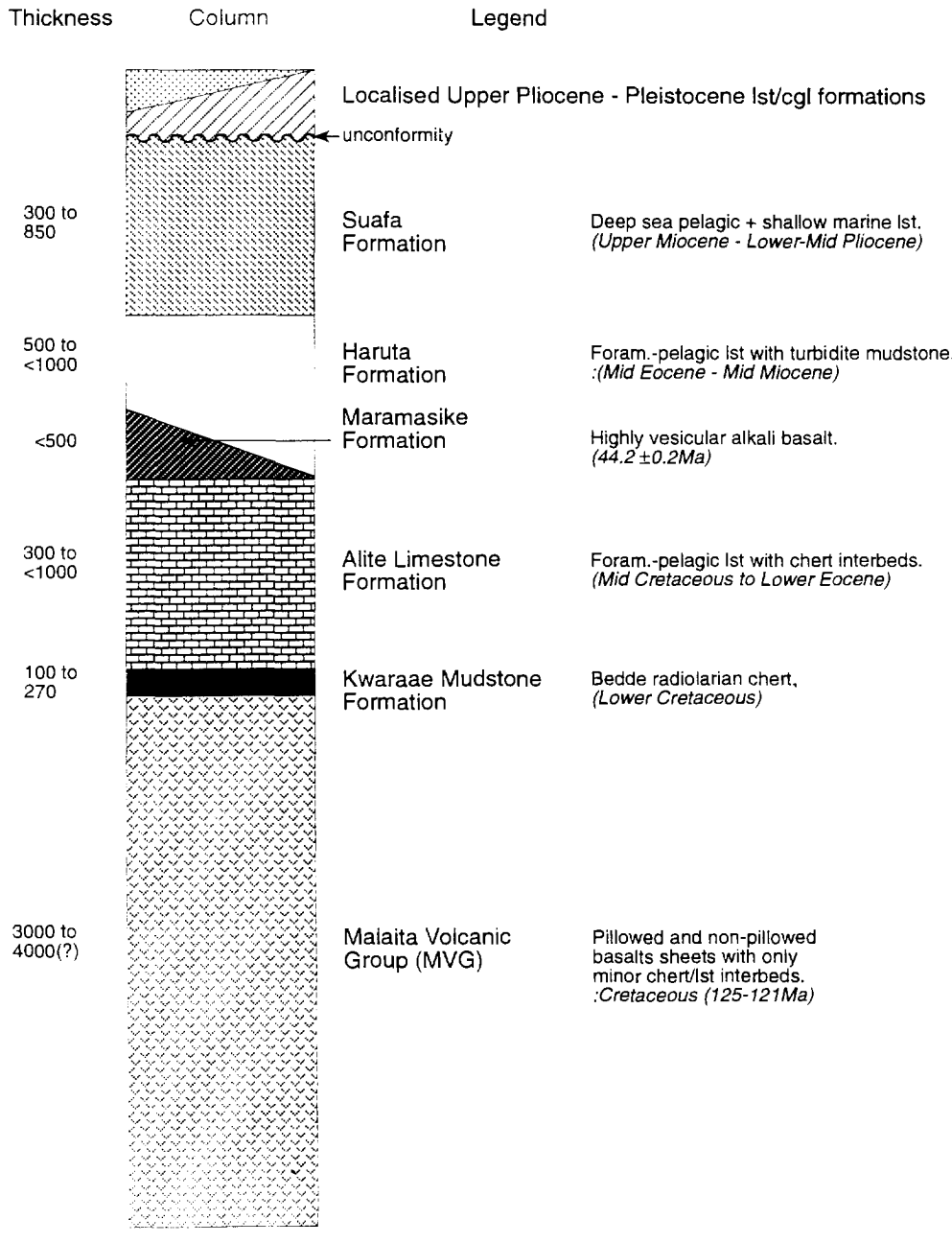

Fig. 3. Generalised stratigraphical column of Malaita essentially comprising of 3–4 km of basement OJP-related basalts and ~1500–3000 km cover sequence dominated by siliceous and calcareous pelagic ooze sediments with localised alkali basalts.

stone Formation. This formation is composed of a parallel-laminated, very fine-grained, radiolarian ± foraminiferal siliceous mudstone. The mudstones become more calcareous in their upper parts. The Kwaraae Mudstone Formation is conformably overlain by the 300–1000-m-thick upper Aptian/lower Albian to Eocene Alite Limestone Formation. Alite Formation limestones comprise an alternating se-

quence of hard, porcellanous, very fine-grained, foraminiferal calcilutites with regular interbeds of chert. The chert/limestone ratio decreases with increasing stratigraphical height. Chert layers are coloured red, white or green, and vary in thickness between 10 and 30 cm, comprising between 15 and 40% of outcrops. The viscosity contrast between the host limestone and chert layers produces a very characteristic structural style dominated by chevron to polyclinal folds, thrusts, boudinage, and pinch and swell structures. Alite Formation calcilutites contain single, double, and multi-chambered foraminifera which comprise between 10% and 60% of individual thin sections. Both the Kwaraae Mudstone and Alite formations contain very low abundances of allochthonous igneous-derived crystals such as plagioclase, vitric grains, etc. The Kwaraae and Alite formations formed as a result of relatively slow pelagic sedimentation within a deep-ocean environment situated at a great distance from any subaerial land mass.

Field data summarised above show that siliceous ooze deposition was predominant or common during MVG, Kwaraae Formation, and lower to middle Alite Formation times (Aptian–Paleocene/Eocene). After this time calcareous ooze deposition became predominant. A simple interpretation of these data is that the local or regional ocean bottom rose in elevation with time from a position beneath the CCD to one above the CCD. However, oceanic lithosphere subsides on cooling, which is in conflict with the interpretation of a rising ocean bottom. Other explanations include:

(1) a deepening of the CCD with time, allowing the carbonate/siliceous ooze ratio to increase despite subsidence of OJP lithosphere;

(2) sedimentation rates high enough to raise the sediment/water interface above the level of the CCD after Maastrichtian to Paleocene/Eocene times;

(3) the earlier lack of carbonate supply reflects a lack of contemporaneous biological productivity;

(4) this portion of ocean floor was approaching a hotspot which caused elevation of the seafloor.

Estimates of CCD depth in the Pacific Ocean (Thierstein, 1979; Arthur et al., 1985) suggest that it was at approximately 3 km depth from 125 to 85 Ma, then increased to 6 km depth at 75 Ma, rebounded back to 3 km at the K–T boundary before returning to 6 km depth during the Paleocene. This supports the general conclusion is that all pre-Upper Miocene sedimentary facies on Malaita are compatible with a deep (>3 km) oceanic origin.

The Maramasike Volcanic Formation, present locally at the top of the Alite Formation, is composed of highly brecciated and vesicular/amygdaloidal alkaline basalts reaching a total thickness of 100–500 m. One sample yielded an Eocene ^{40}Ar–^{39}Ar plateau age of 44.2 ± 0.2 Ma (Tejada et al., 1996). The basalts are both massive and pillowed, with calcite, zeolite, chlorite, epidote, chalcedony, and glass amygdales comprising up to 60% of the total rock volume. Breccias comprise angular basalt clasts set in a glassy or sparry calcite cement. Tachylites, tachylite breccias, and hyaloclastites are common. The predominant mineralogy is clinopyroxene (including Ti-augite), plagioclase, glass, ± olivine, ± apatite. Maramasike basalts display typical alkaline basalt-normalised trace-element patterns, and have $Na_2O + K_2O$ abundances of 3–4%; isotopically some samples are similar to basalts from Raratonga and Samoa, whereas others are similar to OJP lavas (Tejada et al., 1996). The high levels of vesicularity in the Maramasike basalts contrast markedly with the very low vesicularity of basement MVG basalts. Although it is impossible to be definitive about the relationship between degree of vesicularity and depth of extrusion, it is unlikely that high levels of vesiculation (>20%) would result from extrusion below a seawater depth of ~3150 m (e.g., Kokelaar, 1982), although this is partly dependent on magma CO_2/H_2O ratios. Another important observation is that the Maramasike basalts are sandwiched between carbonate pelagic ooze sediments indicative of a relatively shallow-water environment. We suggest that the Maramasike basalts were extruded at more intermediate water depths (?2000–2500 m) from a number of small- to medium-sized seamount-like volcanic centres. The position of the volcanic field was structurally controlled, being situated within a series of extensional grabens (Petterson, 1995). This structural control explains the patchy and restricted outcrop pattern of the Maramasike basalts within the Faufaumela basin of northern Malaita (Fig. 4).

The 500–1000-m-thick, Eocene–Mid-Miocene Haruta Limestone Formation conformably overlies the Alite Limestone Formation, or, locally, the Mara-

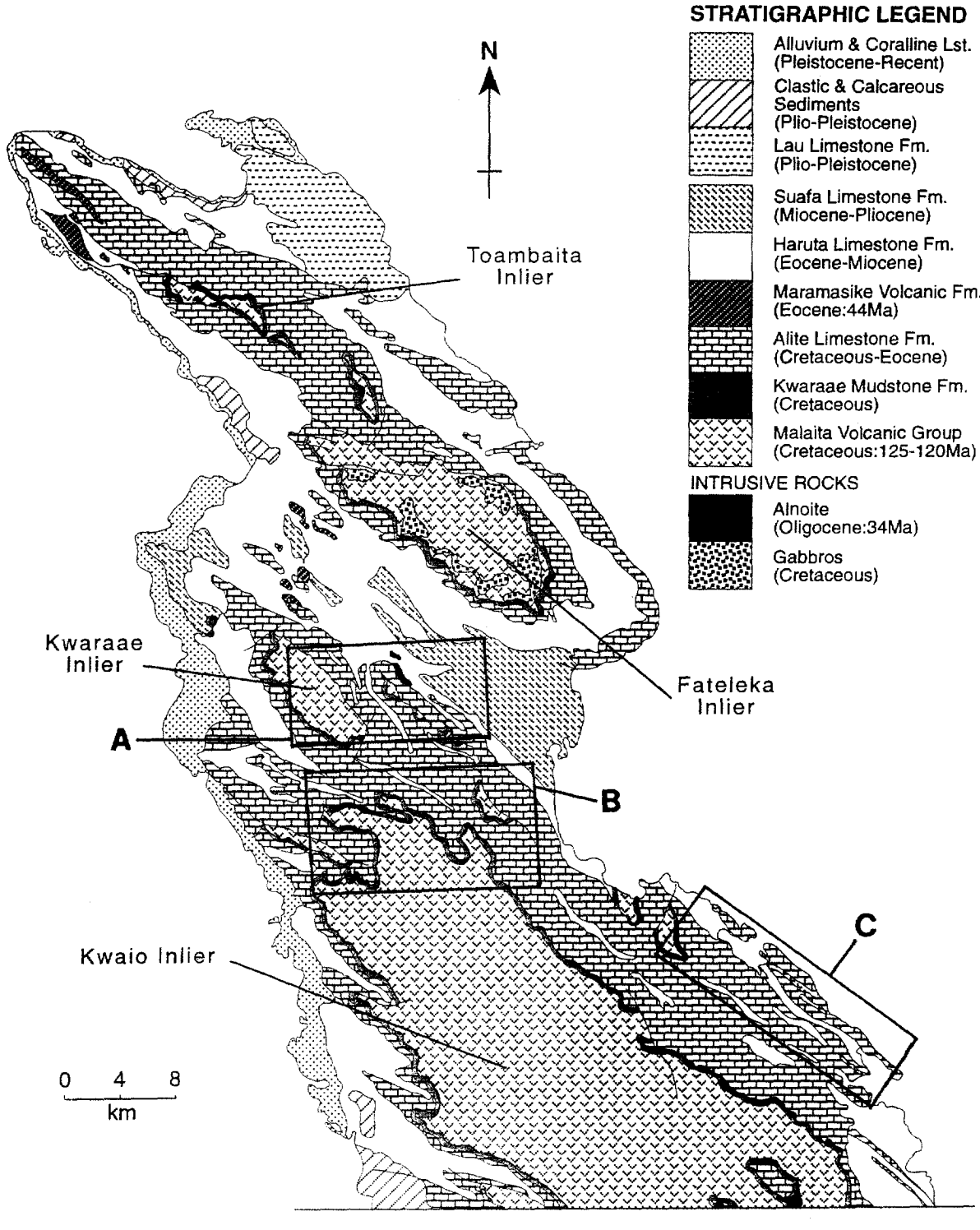
STRATIGRAPHIC LEGEND
Alluvium & Coralline Lst. (Pleistocene-Recent)
Clastic & Calcareous Sediments (Plio-Pleistocene)
Lau Limestone Fm. (Plio-Pleistocene)
Suafa Limestone Fm. (Miocene-Pliocene)
Haruta Limestone Fm. (Eocene-Miocene)
Maramasike Volcanic Fm. (Eocene:44Ma)
Alite Limestone Fm. (Cretaceous-Eocene)
Kwaraae Mudstone Fm. (Cretaceous)
Malaita Volcanic Group (Cretaceous:125-120Ma)
INTRUSIVE ROCKS
Alnoite (Oligocene:34Ma)
Gabbros (Cretaceous)
N
Toambaita Inlier
Kwaraae Inlier
Fateleka Inlier
A
B
C
Kwaio Inlier
0 4 8
km

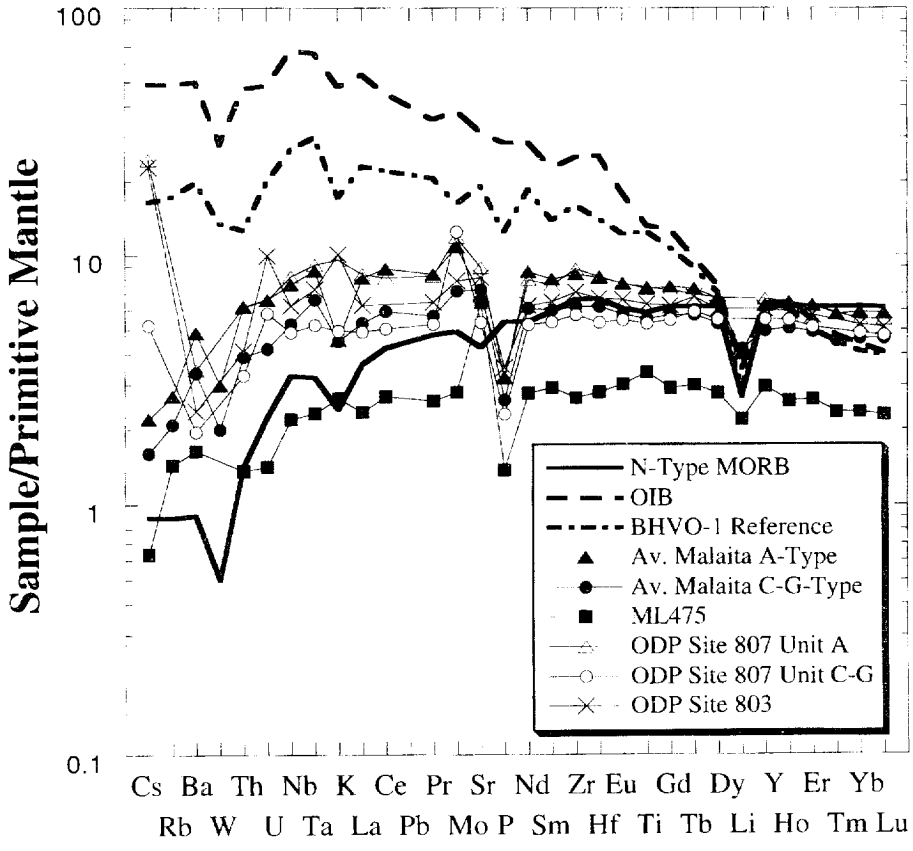

Fig. 5. Comparison of the MVG with the basalts from Ocean Drilling Project boreholes using primitive-mantle-normalised element plots. Note that the Unit A and Unit C–G types from the boreholes are very similar to the A type and C–G types present in the MVG. The Site 803 borehole data tend to be intermediate between the A type and C–G type variants, but these were erupted ~30 Ma later (Mahoney et al., 1993a,b). Basalt ML 475 contains one of the highest MgO abundances (9.99 wt%) of any basalts sampled from Malaita. Primitive mantle values from Sun and McDonough (1989).

masike Volcanic Formation. Haruta Formation sequences are characterised by alternating beds of fine-grained, foraminiferal calcilutites, and dark-coloured turbiditic mudstones, giving the formation a characteristic, striped black and white appearance. The mudstones are typically between <1 and 20 cm thick and display sharp bases and bioturbated tops; they form an excellent way-up criterion. The calcilutite host material contains well preserved foraminifera tests which comprise between 10% and 70% of individual thin sections. Turbiditic mudstones are vitric-crystal-rich and contain shard-like vitric clasts, plagioclase, clinopyroxene and possibly amphibole. Geochemical data indicate a possible basalt-andesite arc provenance for the mudstones (T.L. Babbs and A.D. Saunders, unpubl. data; Petterson, 1995). Structural styles within the Haruta Formation differ from those of the Alite Formation: folds are of a larger

Fig. 4. Geological map of Malaita indicating a remarkable NW–SE structural grain region (the area defined by the box in Fig. 2). Four major basement OJP basalt inliers crop out within major periclinal symmetrical antiforms; these structures are (from south to north): the Kwaio, Kwaraae, Fateleka, and Toambaita inliers. The Auluta thrust belt and Faufaumela basin crop out between the Kwaraae and Fateleka anticlines (see Fig. 7). The areas depicted by the boxes represent sections presented in more detail in later figures; *A* = the Auluta thrust belt, Faufaumela basin, and Fateleka anticline (presented in Fig. 12); *B* = the Fiu re-entrant zone (presented in Fig. 9); *C* = the Sinalanggu area (presented in Fig. 11).

scale, more open, and occasional intra-formational thrusts are present. The Haruta Formation records the input of terrigenous arc material by turbidity currents into a deep-sea, pelagic sedimentary environment, indicating the relative close proximity of subaerial or near-subaerial, volcanic masses.

The 300–850-m-thick, Upper Miocene to Lower–mid-Pliocene Suafa Formation conformably overlies the Haruta Formation. Outcrop distribution of Suafa Formation rocks is highly domainal with the most important locality being the extensional Faufaumela basin (Fig. 4). The Suafa Formation contains a spectrum of litho-facies with one end-member being typical deep-water pelagic limestone, and the other end-member being current-bedded, relatively poorly sorted, calcareous siltstones containing benthonic fauna. Some facies contain up to 10% allochthonous grains (plagioclase, pyroxene, hornblende, biotite, and lithic fragments), reflecting the input of terrigenous volcanic arc material. Suafa Formation sediments were deposited within a basinal environment in both deep and medium-shallow water depths, and in close proximity of landmasses. The Suafa Formation records the gradual emergence of Malaita to near-subaerial levels from its initial deep-water position.

A series of localised Upper Pliocene to Pleistocene clastic sedimentary formations were deposited above the mid-Pliocene unconformity (Figs. 3 and 4). These include:

(1) the calcilutite-dominated Lau Limestone Formation of northeast Malaita;

(2) the brown calcisiltite-dominated Tomba Limestone Formation of northernmost Malaita (Barron, 1993);

(3) the shallow-marine to subaerial, alluvial to deltaic Hauhui Conglomerate Formation of west–central Malaita;

(4) the raised coralline terraces of the Rokera Limestone Formation.

The 34 Ma ultramafic alnöite breccias and finer-grained pipes and sills intrude the Malaitan cover sedimentary sequence as high as Lower Haruta Formation levels (op. cit.). The Malaitan alnöites have a complex mineralogy and can contain olivine, clinopyroxene, melilite, phlogopite, perovskite, spinel, ± nepheline, ± melanite, ± apatite, as well as discrete megacrysts and lherzolitic autoliths (Allen and Deans, 1968; Nixon et al., 1980; Neal, 1985). The location of alnöite intrusions is closely controlled by extensional faults and graben structures. The alnöites formed as a result of small-degree melting of a garnet peridotite (e.g., Nixon et al., 1980) or pyroxenite (e.g., Neal, 1995) at a depth of ~120 km; this melting may have been linked to renewed plume activity, although Coleman and Kroenke (1981) attributed it to the arching of OJP lithosphere over the North Solomon trench.

4. Structural overview

Malaita has only appeared above sea level as an island since the uppermost Pliocene and has a very youthful geomorphology, with relief and coastline all strongly controlled by structure. River and coastline orientations are predominantly parallel or orthogonal to the general NW–SE structural grain, and the areas of highest topographic relief coincide with the basaltic cores of major anticlinal structures.

No evidence exists that the island of Malaita underwent any major phase of compressional deformation prior to the mid-Pliocene transpressive deformational event. The present study indicates that the youngest stratigraphic formation to be deformed is the Suafa Formation, whose age is bracketed by microfaunal and structural evidence at Late Miocene to Early/mid-Pliocene (Hine, 1991; Petterson, 1995). Only the youngest and more localised Upper Pliocene/Pleistocene stratigraphic formations are undeformed and unconformably overlie the deformed Lower Pliocene and older stratigraphic formations. However, it is possible that deformation present within much the larger Malaita anticlinorium region (Fig. 1) may have begun during earlier (?Miocene) times, with the island of Malaita only recording a specific time frame in a deformational continuum which possibly began in the Miocene and continues to the present day.

The fundamental structural characteristic of Malaita is the well developed NW–SE structural grain, emphasised by fold axis orientations (Fig. 6). A more quantitative analysis indicates a modal axial planar strike of 128°. Four major periclinal anticlines are present in north–central Malaita and these are (from north to south) the Tombaita, Fateleka, Kwaraae, and Kwaio anticlines (Figs. 4 and 6).

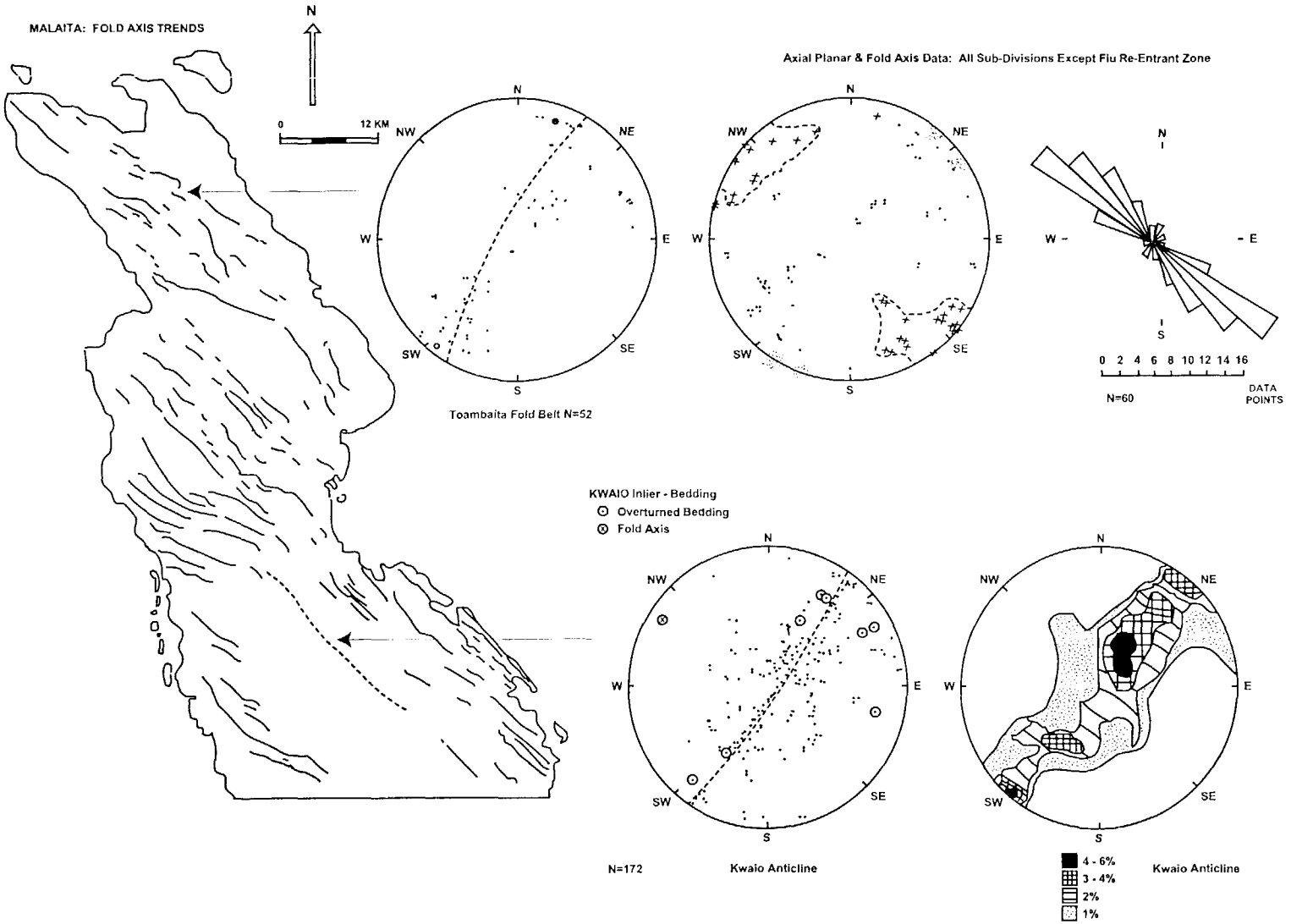

Fig. 6. Map showing fold axial trends of north–central Malaita emphasising the NW–SE structural grain. Note the sigmoidal deviations to the NW–SE trends indicating sinistral-dominated strike-slip. Inset 1 is a stereogram of and *rose diagram* of axial planar and fold axis orientational data for all structural subdivisions except the Fiu re-entrant zone (see also Fig. 7). Note the well developed NW–SE preferred orientation for fold axial planes with fold axes plunging gently NW or SE. Insets are stereograms of bedding orientational data for the Kwaio and Toambaita structural subdivisions (see Fig. 7 for map of structural subdivisions). See text for further details.

All display vergence to the northeast, except the Tombaita anticline which exhibits a southwest vergence. All are asymmetrical and have upright to overturned axial planes (Fig. 6). Sigmoidal deviations to the general NW–SE structural grain are locally present (e.g., northern edge of the Kwaio anticline and within the Tombaita structure; Figs. 6–8). Also, the large NE-verging folds are locally refolded about later southwest-verging folds (e.g., the Kwaio back thrust belt; Figs. 6 and 7). In addition, the Fiu re-entrant zone (Fig. 9) is discordant with the general structural grain of Malaita. Structures within this zone subtend at an angle ~20° anticlockwise to the regional strike, with the whole structure indicating a sense of sinistral strike-slip movement.

Thrust faults present on Malaita (Fig. 8) are oriented NW–SE with a minor N–S and E–W component. The majority of thrusts dip to the southwest and south with a minor northeast-dipping population (generally restricted to the Kwaio backthrust belt). The thrust faults give a sense of movement to the northeast, but when combined thrust movement and minor fold vergence are considered, it is apparent that although a northeast sense of movement predominates, there is a significant sense of movement recorded in the opposite direction. Field relations demonstrate that the predominant northeast vergence and sense of thrust movement predates the southeast vergence event.

The major faults present on Malaita have predominant NE–SW orientations and suggest at least four major events (Fig. 10); the earliest of these was probably related to the formation of the OJP. The second event was related to a period of extension and basin formation during the Eocene/Early Pliocene which formed WNW–ESE- and NE–SW-trending faults. This period of extension was followed by mid-Pliocene compression, again producing ESE–WNW- and NW–SE-trending faults as well as reactivating earlier ones. The final fault-forming event (Upper Pliocene to present) produced faults of a variety of orientations (particularly NE–SW and E–W), possibly as a result of pressure release and uplift.

The existence of the regional NW–SE structural grain, together with the sigmoidal fold structures, are interpreted as reflecting a general NE–SW-directed (038–218°) compressional event with simultaneous, predominantly (though not exclusively) sinistral strike-slip. These tectonic features reflect a transpressional phase of deformation consistent with the present-day oblique convergence of the Pacific and Australian plates (Figs. 1 and 2). The structural data (Fig. 6) are further interpreted as reflecting a Lower to mid-Pliocene tectonic event which physically moved material towards the northeast, followed by a later backthrusting tectonic style with resultant thrusting towards the southwest. This interpretation is corroborated by seafloor swath mapping data adjacent to Malaita (e.g., Kroenke, 1995).

4.1. Structural subdivisions

It is possible to divide north–central Malaita into a number of subdivisions which have a common structural style and/or illustrate unique structural characteristics. This approach is particularly useful with respect to a quantitative analysis of structural data. Line-balanced cross-sections using the relatively thin Kwaraae Mudstone Formation as the template horizon (e.g., Ramsay and Huber, 1987) are generally drawn perpendicular to the local strike, and use field traverse data and local dips to constrain structural models. The deeper structural models presented in line-balanced and other sections (Fig. 7) indicate that the large asymmetrical fold structures are blind tip regions of thrusts which have a detachment surface 1–4 km beneath the basement–cover transition plane. The blind thrust model is the preferred conceptual model for the Malaitan folds as it explains their geometry and vergence, the close relationship between folding and thrusting in some areas, is a plausible mechanism for explaining the overall shortening of Malaita, and accords well with the regional structure of the Malaitan anticlinorium imaged by numerous seismic and swath mapping surveys (these reveal a regional thrust stack-foreland basin structure, e.g., Sopacmaps, 1994; Kroenke, 1995). The subdivisions combine to make up approximately one third of the area of north–central Malaita (Figs. 4 and 7) and the important features of the structural subdivisions areas are discussed below from south to north.

4.1.1. Kwaio anticline — Kwaio backthrust belt — Sinalanggu fold belt subdivisions

The Kwaio anticline is the largest single fold structure present on Malaita (Fig. 4). It has a NW–

SE-trending long axis measuring some 65 km, a half wavelength of 17 km, and vergence is to the northeast. A cross-section through the southern part of the Kwaio anticline extending into the Sinalanggu fold belt (Fig. 7a) illustrates the asymmetrical, slightly overturned nature of the large Kwaio anticline fold axis, with three NE-directed thrusts present along the western limb of the fold. The fold belt is composed of a number of short-wavelength fold structures which form part of a larger-scale synformal structure. Fold vergence is symmetrical (to the northeast and southwest) about the central Sinalanggu fold structure.

A section through the Kwaio backthrust belt, the Kwaio anticline, and the northern part of the Sinalanggu fold belt (Fig. 7b) demonstrates that the western limb of the Kwaio anticline has undergone a later phase of refolding and backthrusting. This late-stage deformational phase includes both southwest fold vergence and southwest-directed thrusting. Later SW-directed thrusts are seen cutting their earlier NE-directed counterparts (Fig. 7b). The northern part of the Sinalanggu fold belt comprises NE-verging, overturned, asymmetrical folds.

A line-balanced cross-section through the northern part of the Kwaio anticline (Fig. 7c) is drawn orthogonal to the predominant shortening direction, close to actual geological field traverses. Section-balancing calculations for Fig. 7c demonstrate that:

(1) this part of Malaita has undergone 15–16 km (or 36%) of shortening;

(2) 3.5–4 km of basement basalts have been folded by the Kwaio anticline;

(3) the major detachment surface is situated at a depth of 3.5–4 km beneath the cover sequence;

(4) this section (along with several others in Fig. 7) suggests that smaller-scale thrusts which break surface probably 'root' at the deeper 'master' detachment surface.

Folds of the Sinalanggu fold belt are well defined by the alternating outcrops of Haruta and Alite Limestone formations (Fig. 11) and this belt is an excellent example of the style of deformation present in the cover sequence of Malaita. Key elements of this structural style include:

(1) an average fold wavelength of 1.0–1.5 km;

(2) a predominant NW–SE fold axial trace direction;

(3) sigmoidal outcrop traces for many of the Haruta Limestone outcrops demonstrate that the area has undergone a degree of predominantly sinistral strike-slip deformation;

(4) areas of overturned strata are present;

(5) NE–SW-trending faults dominate.

4.1.2. Fiu re-entrant zone

The Fiu re-entrant zone marks the change in structural grain from NW–SE within the northern part of the Kwaio anticline to WNW–ESE just to the north (Figs. 4, 7 and 9). This zone represents the largest area of north–central Malaita with a consistent structural discordance to the predominant NW–SE structural grain. The area is dominated by folds with a wavelength of ~3–10 km, which represent the northern terminal zone of the Kwaio anticline and related parasitic folds superimposed on the limbs of the larger Kwaio structure. The sigmoidal axial fold traces reflect local strike-slip movements which are predominantly, but not exclusively, sinistral. The eastern part of this subdivision has experienced considerable shortening, illustrated by a number of north-directed thrusts (Fig. 9). Stereographic projections of bedding orientational data (Fig. 9) define more symmetrical fold morphologies with SSW-vergence and a general fold axial plunge of 3–108°.

4.1.3. Auluta thrust belt, Faufaumela basin, and Fateleka anticline

In these subdivisions, NE-verging faults predominate, with a modal fold axis plunge orientation of 6–129° (Fig. 12). The presence of two population maxima in the SW quadrant of the bedding orientation stereogram presented in Fig. 12 demonstrates that strike-slip movements have locally affected these areas.

The Auluta thrust belt is perhaps the most complex area structurally, as it has experienced the largest degree of shortening in central–northern Malaita. This is demonstrated by the high density of imbricated thrusts (Fig. 7d–g) which shows movement predominantly to the northeast and involves both basement and cover rocks. Asymmetrical, overturned folds with a predominant NE-vergence are closely associated with these thrusts. Indeed, many of these folds have thrusted northern limbs. Fold

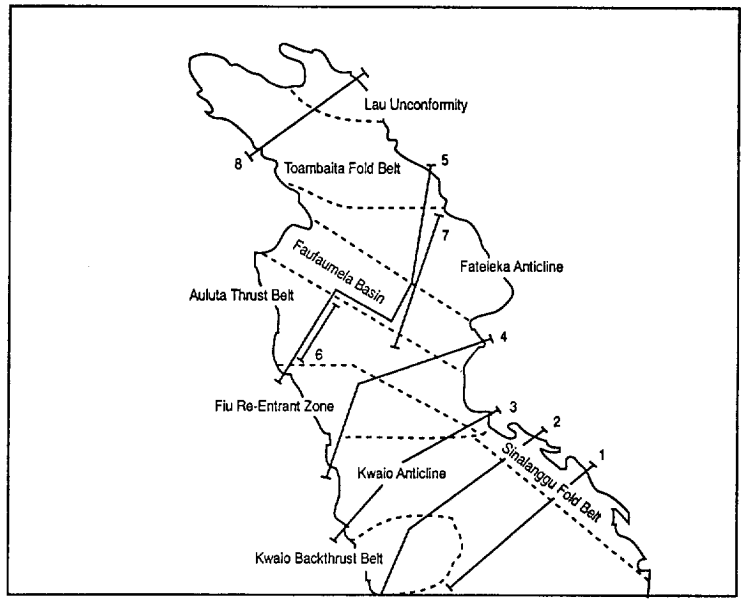
Lau Unconformity
Toambaita Fold Belt
Faufaumela Basin
Fateleka Anticline
Auluta Thrust Belt
Fiu Re-Entrant Zone
Kwaio Anticline
Sinalanggu Fold Belt
Kwaio Backthrust Belt
1
2
3
4
5
6
7
8

(a)

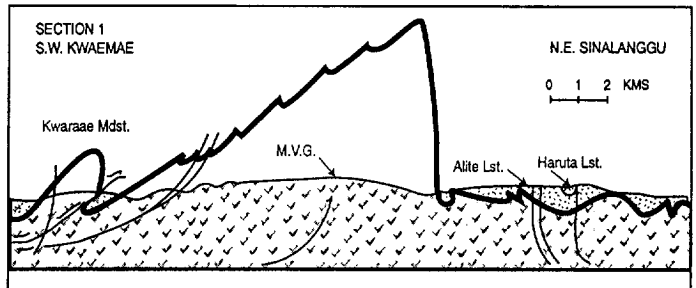
SECTION 1
S.W. KWAEMAE
N.E. SINALANGGU
0 1 2 KMS
Kwaraae Mdst.
M.V.G.
Alite Lst.
Haruta Lst.

(b)

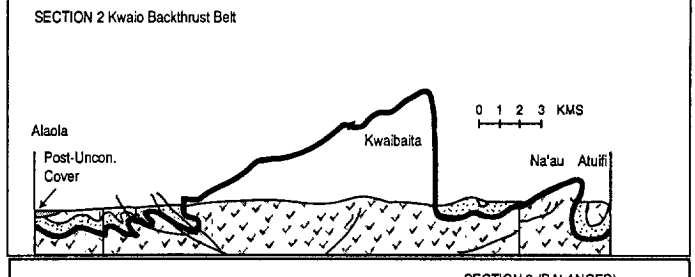
SECTION 2 Kwaio Backthrust Belt
0 1 2 3 KMS
Alaola
Post-Uncon.
Cover
Kwaibaita
Na'au
Atuifi

(c)

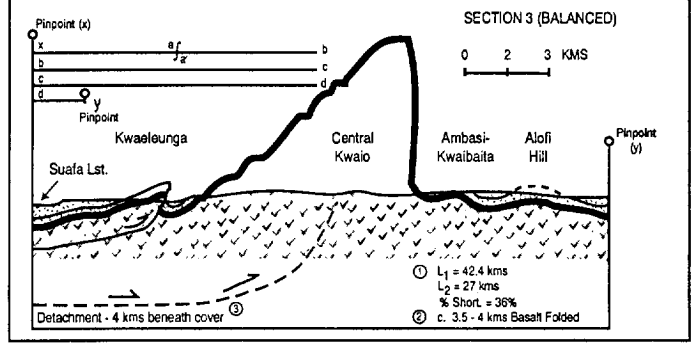
Pinpoint (x)
SECTION 3 (BALANCED)
0 2 3 KMS
Pinpoint
Kwaeleunga
Central
Kwaio
Ambasi-
Kwaibaita
Alofi
Hill
Pinpoint
(y)
Suafa Lst.
① L1 = 42.4 kms
L2 = 27 kms
% Short. = 36%
② c. 3.5 - 4 kms Basalt Folded
Detachment - 4 kms beneath cover ③

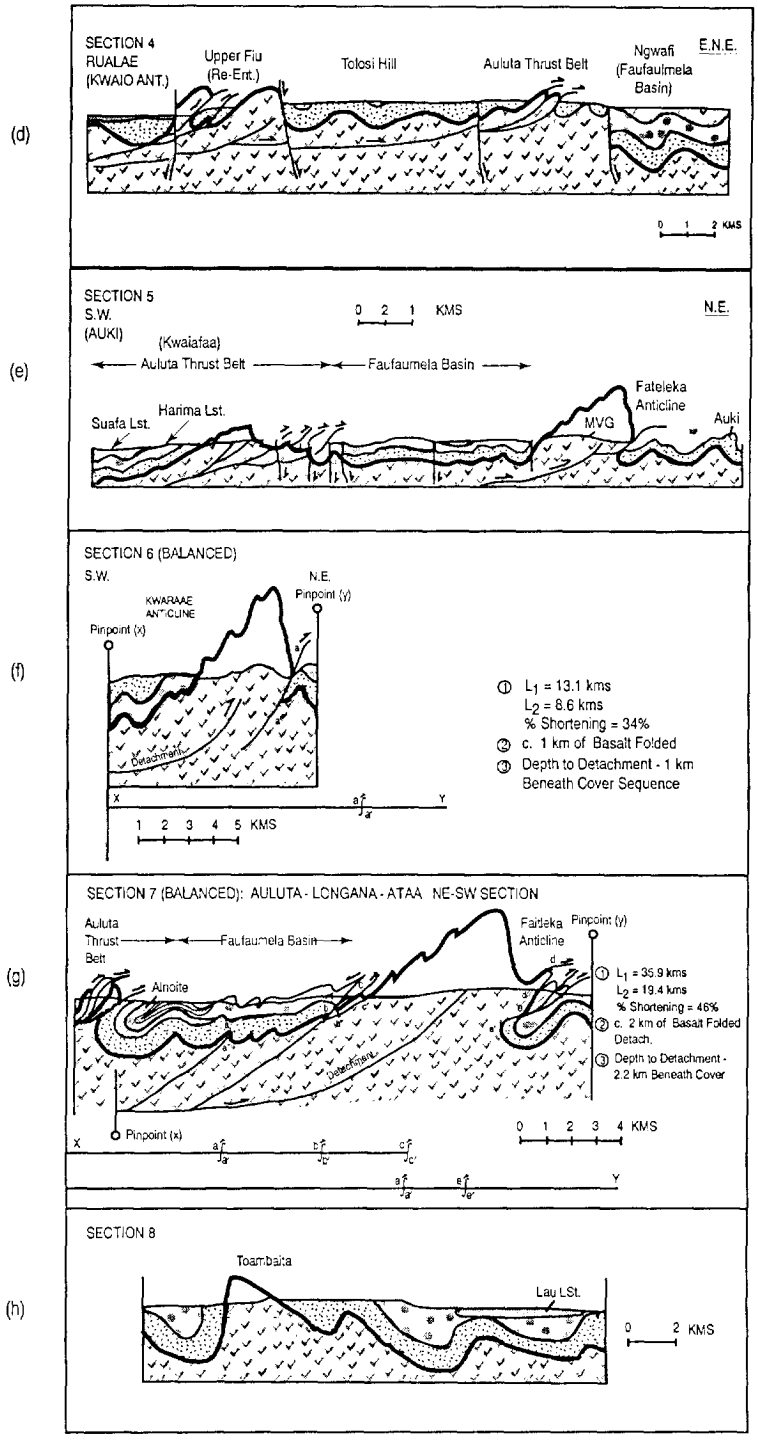

Fig. 7. Geological cross-sections through north–central Malaita. Lines of section and structural subdivisions of Malaita are shown on the inset map. Sections (e), (f), and (g) are line-balanced using the Kwaraae Mudstone Formation as a structural template. Pinpoints indicate terminal positions of line-balancing calculations. Sections indicate original and final lengths of the template formation (L_1 and L_2, respectively), the total % shortening, maximum thickness of basalt involved in folding, and estimated depth beneath the cover sequence to the postulated major detachment.

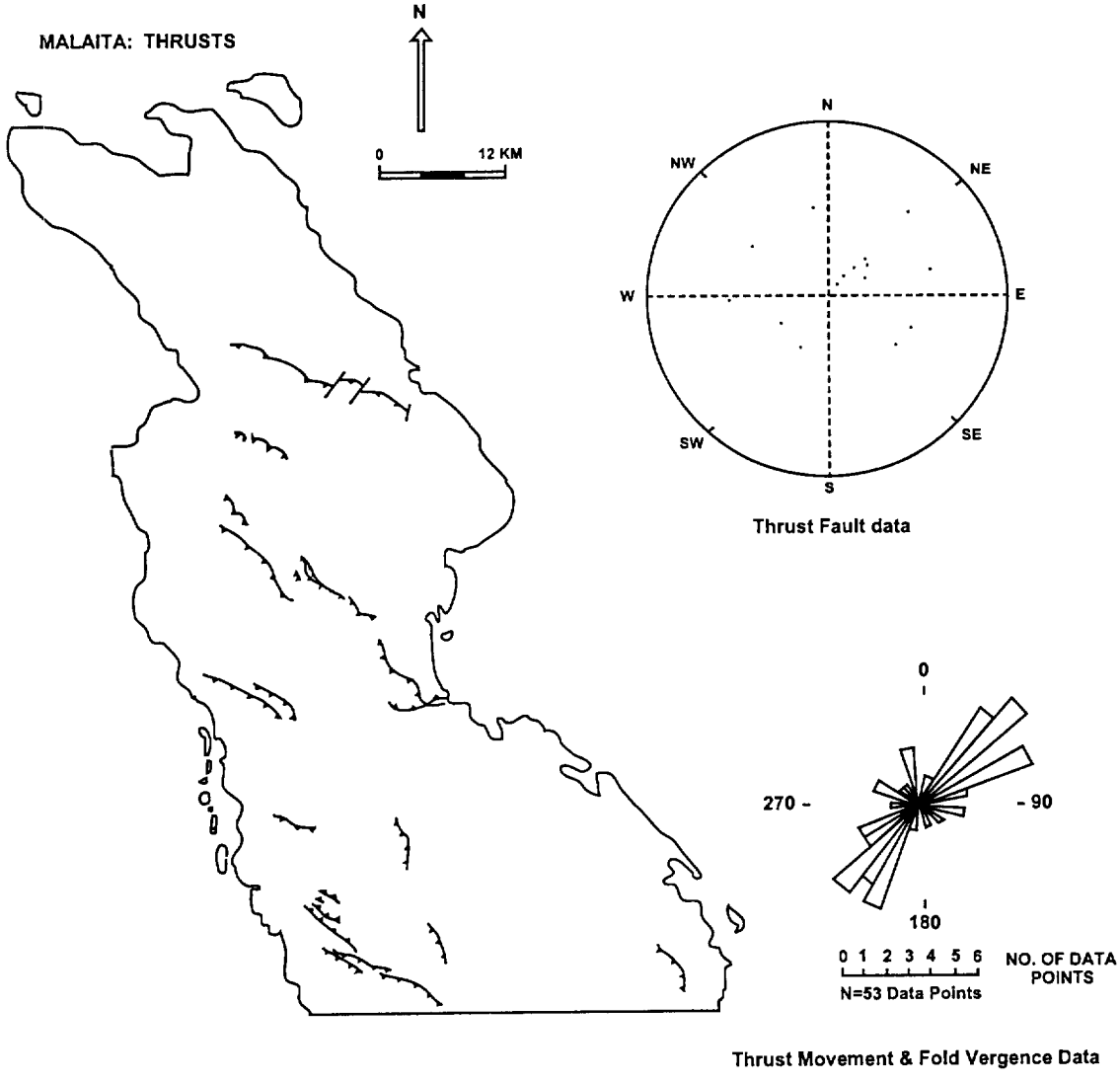

Fig. 8. Map of thrust fault orientations in north–central Malaita indicating the predominant NW–SE strike and southwesterly dip except in the Kwaio backthrust zone where a number of northeasterly dipping thrusts crop out. Teeth are situated on the hanging wall. Insets show stereographic projections of thrust plane orientational data and a rose diagram presentation of thrust movement direction and fold vergence direction data. See text for details.

wavelengths vary between 500 m and 3 km (e.g., Fig. 7d,e,g, and Fig. 12). A line-balanced cross-section through the northern part of the Auluta thrust belt, the Faufaumela basin, and the Fateleka anticline demonstrates the general overturned nature of the folds and the NE-vergence of fold and thrust structures (Fig. 7g). This section clearly demonstrates the sympathetic relationship between the Auluta syn-

Fig. 9. Geological map of the Fiu re-entrant zone emphasising the change in orientation of fold axes from NW–SE to WNW–ESE, and SE-dipping thrust faults with a NE-sense of displacement. Insets are stereographic projections of bedding and axial planar/fold axis plunge data and a rose diagram of axial planar strike for the Fiu re-entrant zone. Note the 20° anticlockwise angular discordance between the Fiu re-entrant zone and the general structural trend of Malaita. See Fig. 4 for location in north–central Malaita.

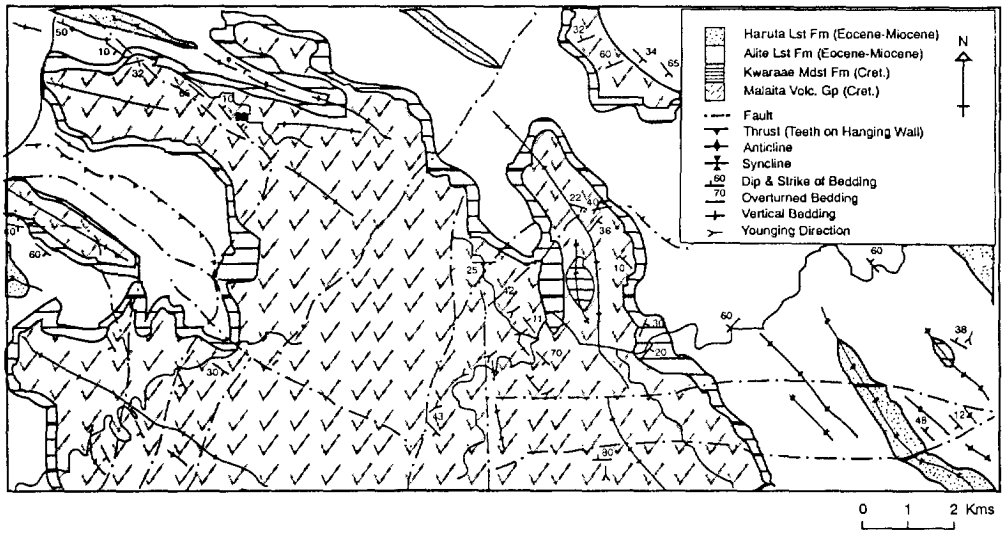

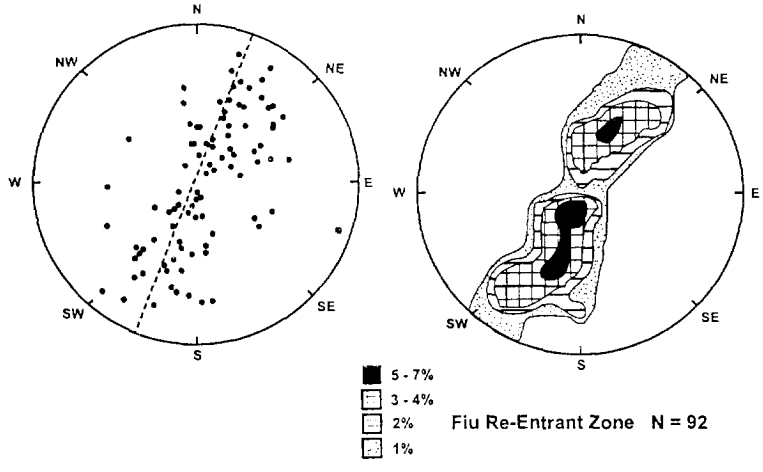

Axial Planar & Fold Axis Data: Fiu Re-Entrant Zone

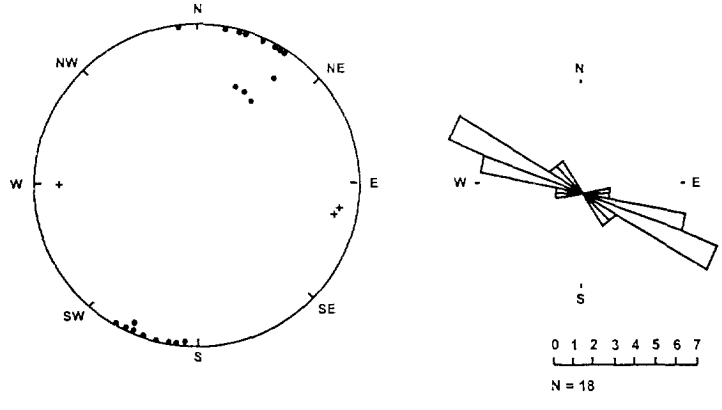

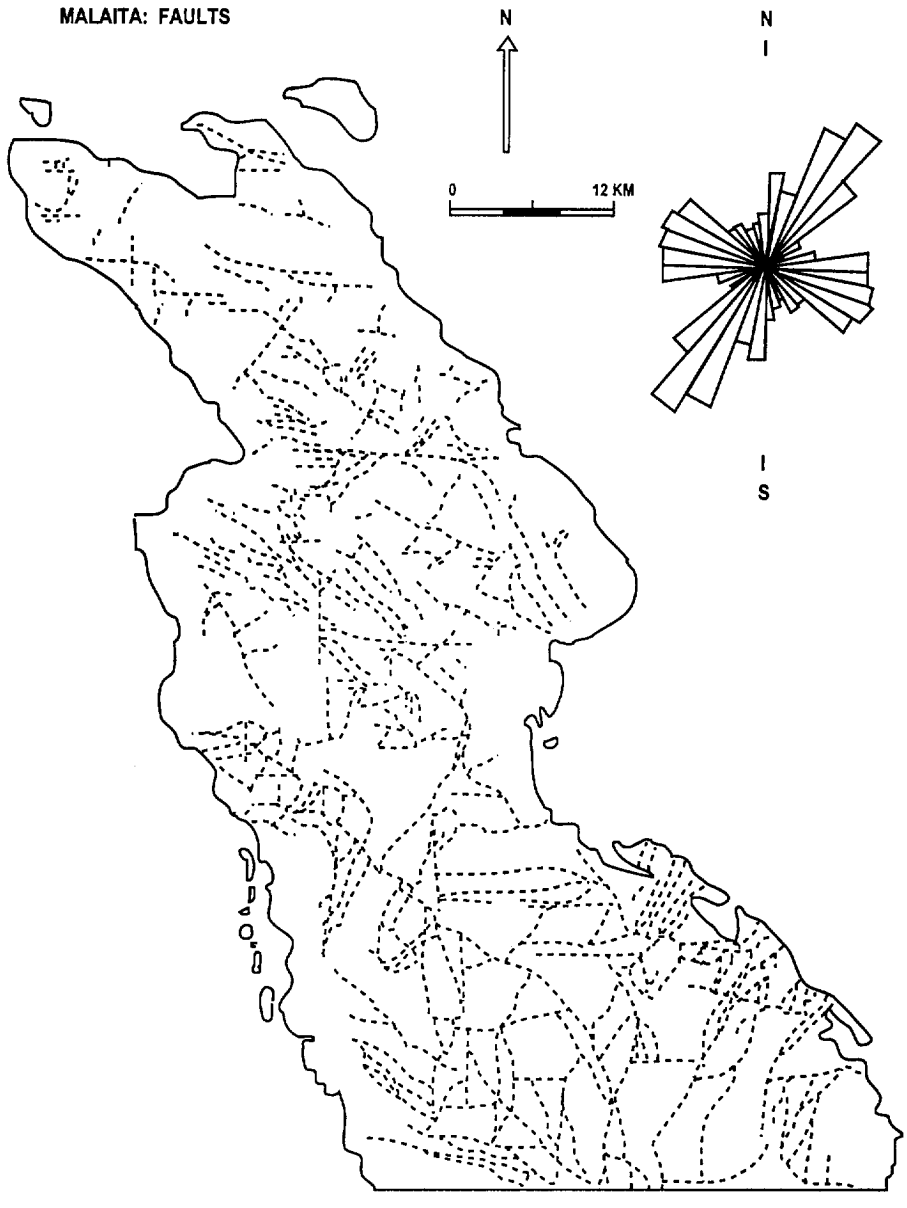

Fig. 10. Map of fault trends in north–central Malaita. Inset diagram is a rose diagram of fault strike data indicating predominant NE–SW, ESE–WSW, and N–S preferred orientations.

cline and the complementary Fateleka anticline; this complete structure has a wavelength of ~17 km. The Fateleka anticline is thrusted along its northern, overturned limb and this has a very strong photo-geological expression. Analysis of photo-lineaments in this area suggests that the northern edge of the Fateleka anticline has experienced (?strike-slip) rotational, movements in addition to the NE-verging thrust movements. Calculations based upon line-balancing of this section demonstrate that:

(1) the area has experienced a total of 16.5 km (46%) of shortening; this relatively high-percentage shortening reflects the fact that much of the shortening has been accommodated by thrusting;

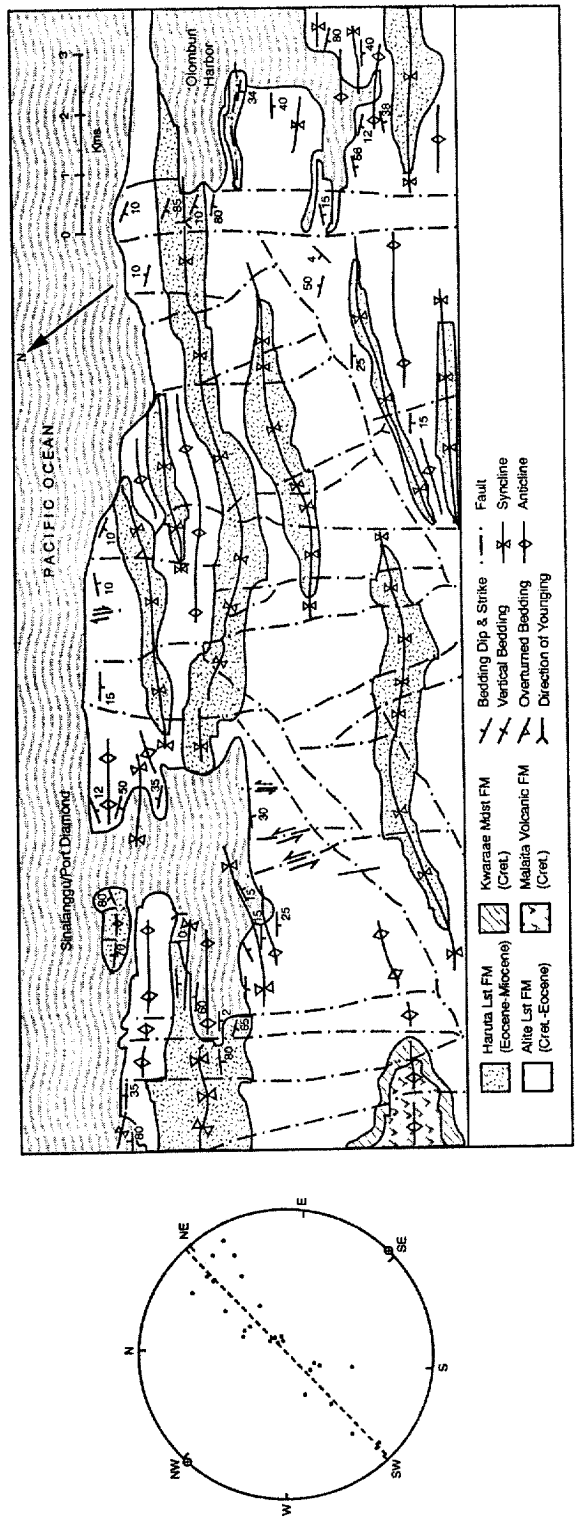

Fig. 11. Geological sketch map of the Sinalanggu area showing folded repetitions of alternating outcrops of cover limestone formations. Inset is a stereogram of bedding orientational data for the Sinalanggu area. See text for details and Fig. 4 for location in north–central Malaita.

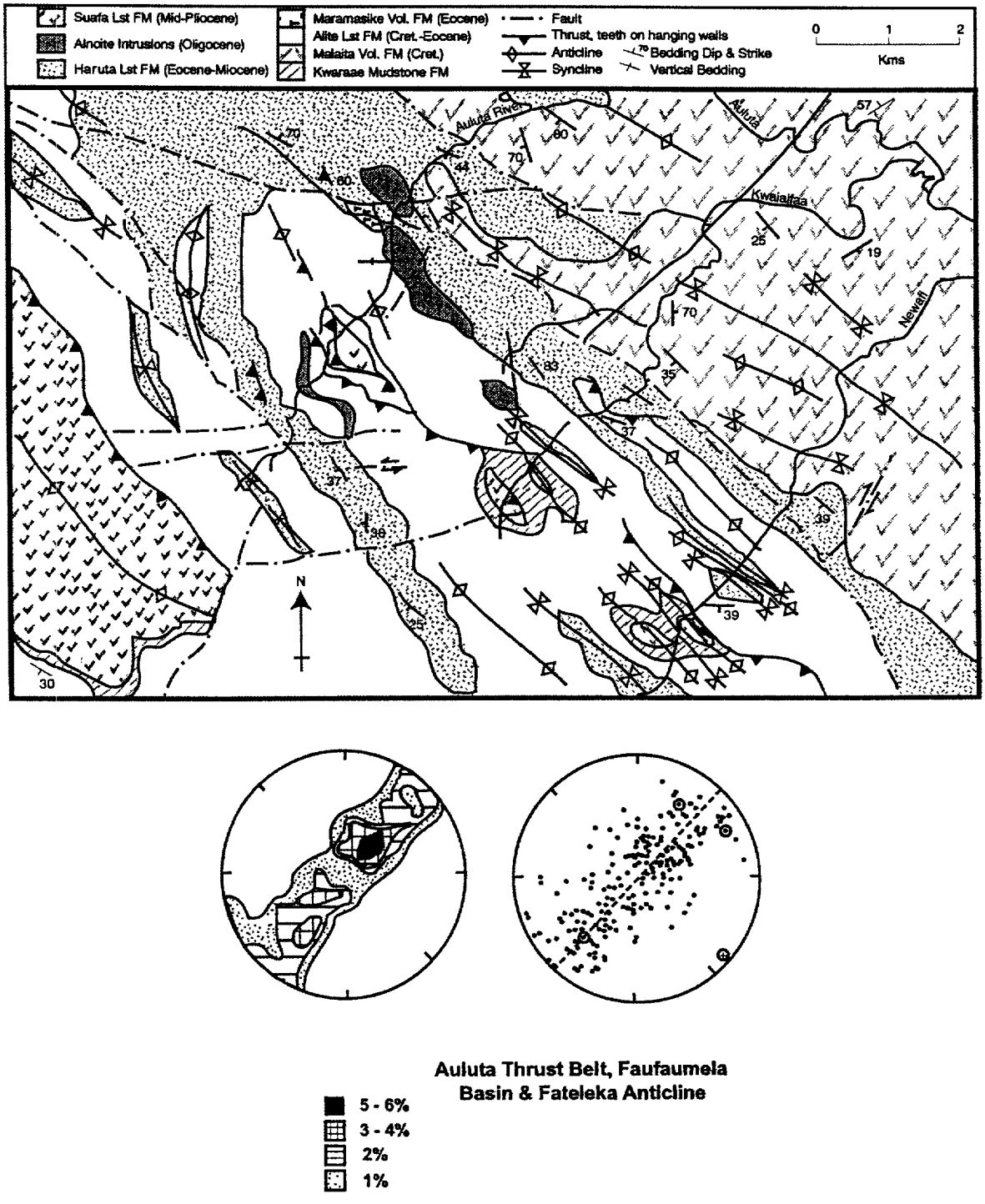

Fig. 12. Geological sketch map of part of the Auluta thrust belt, Faufaumela basin, and Fateleka anticline with inset stereogram of bedding orientational data of this area of Malaita. See text for details and Fig. 4 for location in north–central Malaita.

(2) approximately 2 km of basement MVG basalts have been folded by the Fateleka anticline;

(3) the major detachment zone to the Fateleka anticline is calculated to be situated at a depth of 2 km beneath the cover sequence; smaller-scale thrusts root from this major detachment.

A line-balanced cross-section across the Kwaraae anticline (Fig. 7f), situated in a less deformed part of the Auluta thrust belt, demonstrates that:

(1) this area has experienced a total of 4.5 km (34%) absolute shortening;

(2) approximately 1 km of basement MVG basalts have been folded by the Kwaraae anticline;

(3) the major detachment surface to the Kwaraae anticline is estimated to be at a depth of 1 km beneath the cover sequence.

The general structure of the Faufaumela basin is illustrated in Fig. 7d,e,g). The Ngwafi area (Fig. 7d) is underlain by a thickened pelagic sedimentary sequence dramatically thickened on the downthrown basinal side of a major (normal) growth fault. The Ngwafi fault has an apparent throw of ~1.5 km, but was probably re-activated as a reverse fault in mid-Pliocene times; before the mid-Pliocene deformation the throw of the Ngwafi fault was probably even greater. The Faufaumela basin is essentially a synformal structure which plunges to the southwest (Figs. 4 and 7). This area has been a region of extension and basin formation since Eocene times with deep-level basement structures controlling overall structural development; four key pieces of evidence lead to this conclusion.

(1) This area is one of only two areas in north–central Malaita which contains outcrops of the Eocene alkaline basalts of the Maramasike Volcanic Formation. The Maramasike Formation basalts are sandwiched stratigraphically between the Cretaceous–Eocene Alite Limestone Formation and the Eocene–Miocene Haruta Limestone Formation. A probable tectonic setting for the eruption of these basalts is within an extensional depo-centre, with the deep-sourced magma utilising basement structures to rise to surface eruption sites.

(2) The Oligocene alnöites crop out exclusively within the Faufaumela basin and the northern part of the Auluta fold belt. These are ultramafic magmas of deep-seated origin which again have probably risen along deep-basement extensional faults which in turn control basin development in the Faufaumela basin area.

(3) This area contains by far the thickest sequence of the Miocene–Pliocene Suafa Limestone Formation, and a thickened sequence of the Eocene–Miocene Haruta Limestone Formation. Sedimentation rates increased with time, with a maximum sedimentation rate occurring during Suafa Formation times (Late Miocene to Early/mid-Pliocene). Sedimentation rates are inversely proportional to water depth in deep-water pelagic environments far removed from terrigenous sediment input (e.g., Berger et al., 1992). Combined structural and sedimentation rate evidence implies that the Faufaumela basin was a graben structure within a relatively elevated part of the Ontong Java Plateau.

(4) Elevated concentration levels of heavy metals, in particular Ag and Pb, in stream sediments from the Faufaumela basin (Mahoa and Petterson, 1995), can easily be explained by the activity of hydrothermal cells related to the magmatism present within the basin. The presence of extensional faults would greatly facilitate mineralisation.

4.1.4. Toambaita fold belt — Lau unconformity subdivisions

This area is the most poorly known area in terms of field data because access is limited in the hinterland of the island. However, a cross-section through this area (Fig. 7h) demonstrates the general fold morphology with fold vergence to the southwest; this is the opposite of the predominant NE-vergence of Malaitan folds. Bedding orientational data for the Toambaita anticline demonstrate the steeply dipping to overturned character of rocks on both limbs, particularly in the southwest (Fig. 7). The fold axis plunges towards the east-southeast, somewhat discordant to the regional NW–SE structural grain. The Fateleka anticline exhibits NE-vergence and is in close proximity to the Toambaita anticline, which implies that the intervening syncline has been essentially thrusted out. Calculations based on Fig. 7h suggest that the area has experienced approximately 24% of crustal shortening.

4.1.5. Summary

The main conclusions of the structural study from Malaita are as follows:

(1) The topography of Malaita is youthful and strongly controlled by structure.

(2) Rocks that vary in age from Cretaceous to Early/mid-Pliocene have been affected by the same phase of compressive to transpressive deformation, and form a structurally coherent sequence.

(3) Upper Pliocene to Pleistocene and Recent sediments unconformably overlie the older, deformed sequence.

(4) The age of compressive–transpressive deformation is stratigraphically bracketed between the Lower/mid-Pliocene and Upper Pliocene *on the island of Malaita*. It is possible that the regional compressive deformation which affected the much larger Malaita anticlinorium region began during earlier Miocene times.

(5) There is a strongly developed structural grain with an average strike of 128°.

(6) Some areas are locally discordant to the 128° strike direction; the angular discordance is up to 20° anticlockwise and reflects strike-slip movements which are predominantly, but not exclusively, sinistral. This strike-slip deformation was essentially penecontemporaneous with the mid-Pliocene compressive deformation: thus the mid-Pliocene deformation was *transpressive* in character.

(7) Malaitan thrusts and asymmetrical fold structures have resulted from NE–SW compression with accompanying transpression, and show a predominant sense of movement/vergence to the northeast. A subsequent SW-directed backthrust phase of deformation is recognised.

(8) Although both volcanic basement and sedimentary cover sequences are involved in folding and thrusting deformation, there is no major decollement surface between them.

(9) The large anticlines present on Malaita are the result of blind thrusts which have detachment surfaces of between 1 and 4 km beneath the sedimentary cover sequence. Similar thicknesses of basement (1–4 km) are involved in the folds/thrust structures.

(10) Line-balanced cross-sections indicate local crustal shortening of between 24% and 46%.

(11) The Faufaumela basin has been a depo-centre since at least Eocene times with sedimentation rates in the basin increasing with time. The basin has also been a focus for alnöite and alkaline basaltic intrusion and extrusion. Constructed, scaled, geological cross-sections indicate the presence of basin-margin extensional growth faults with downthrows of ~1.5 km. A combination of sedimentation rates and structural evidence suggests that the Faufaumela basin has been a graben structure located within a structural high region of the Ontong Java Plateau for a considerable part of the area's history.

5. Ontong Java Plateau–Solomon arc collision

5.1. Formation of OJP and subsequent passive drift northwards

The OJP formed above a major Cretaceous plume head in the southern Pacific, between 35° and 50° south, with major plateau-building magmatic events at ~122 Ma and 90 Ma (e.g., Mahoney et al., 1993a,b; Tejada et al., 1996; Neal et al., 1997). The portion of the OJP that now forms Malaita probably formed along the southern edge of the plateau thousands of kilometres away from the position of the present-day Solomon Islands. From the Aptian to the Mid-Eocene the cover sequence of Malaita records deep-water pelagic sedimentation within an intra-oceanic environment. This is interpreted as the southern part of the OJP being passively carried northwards as part of the Pacific Plate. During the Eocene the Pacific Plate began to subduct beneath the Australian Plate at the North Solomon/Vitiaz trench which resulted in Stage-1 arc activity along a northeast-facing Solomon arc (e.g., Kroenke, 1984). The Eocene was also a period of change within the cover sequence of Malaita. This change commenced with the eruption of the highly vesicular alkaline Maramasike Formation basalts which may have been erupted as the OJP passed over the Samoan, or possibly Raratongan hotspot (Tejada et al., 1996). The high vesicularity of the Maramasike basalts contrasts markedly with the distinct lack of vesicularity of the OJP-related Malaita Volcanic Group tholeiitic basalts and indicates a shallower-submarine eruptive setting, possibly from a series of seamounts. The eruption of the Maramasike basalts marks the beginning of a period of extension within the southern OJP which resulted in the development of the Faufaumela basin. Basin development was controlled by crustal-scale extensional structures which allowed for the ingress of magmas relating to both the eruption of

the Maramasike volcanic rocks and intrusion of the Oligocene alnöites, and the development of thickened Eocene–Lower Miocene sediments within the basin. From the Mid-Eocene to the Mid-Miocene, cover sediments on Malaita also record a high percentage of arc-related volcaniclastic turbidites which indicate that the southern OJP was by this time relatively close to sediment-charged turbidite fans probably originating from the Stage-1 Solomon arc.

5.2. First contact between the OJP and Solomon arc

The timing of the first contact between the OJP and the Solomon arc is controversial but is generally bracketed between ~25 and 20 Ma and related to the cessation of Stage-1 arc volcanism (e.g., Coleman and Kroenke, 1981; Kroenke, 1984; Yan and Kroenke, 1993). If correct, the age of the youngest dated igneous rock relating to the Stage-1 arc limits the timing of the first contact (24 ± 0.4 Ma for the Poha diorite of Guadalcanal; Chivas, 1981). Initial contact of the OJP with the Solomon arc did not result in any major compressional event within the plateau; the cover sequence from Malaita during the Early and Mid-Miocene does not record any significant uplift or any compressive tectonism. Thus, this initial contact was a 'soft docking' (Fig. 13; Table 1) in the sense that the deformational front did not extend to the future island of Malaita.

5.3. Subduction-related tectonics along the Vitiaz and South Solomon trench systems from 25 Ma to the present

Although subduction ceased along the Vitiaz trench in the vicinity of Solomon Islands during the Early Miocene, it appears to have recommenced during the Mid-Miocene (from ~15 Ma), and has continued intermittently and locally to the present day. Evidence to support this assertion includes:

(1) The arc-related volcanic centres of Maetambe and Komboro on Choiseul were active during the Mid-Miocene and Pliocene, respectively (Ridgeway and Coulson, 1987; Fig. 13; Table 1). Choiseul is at a much more typical arc–trench gap distance with respect to the Vitiaz trench relative to the SSTS, especially as the great bulk of the volcanic centres related to the SSTS are situated anomalously close to the trench compared to most arc systems (e.g., Johnson and Tuni, 1987; Johnson et al., 1987; Petterson, 1995).

(2) Present-day seismicity within the vicinity of Solomon Islands indicates that active subduction with a southwestern polarity is taking place beneath Santa Isabel. This subduction is related to the Vitiaz trench (Cooper and Taylor, 1984; Cooper et al., 1986; Petterson, 1995).

(3) Recent swath mapping of the ocean floor between Makira (formerly San Cristobal), and Santa Cruz revealed numerous volcanic edifices oriented along three linear to arc-shaped chains (Sopacmaps, 1994; Kroenke, 1995). The southernmost chain is related to northwards-directed subduction of the Australian Plate beneath the Solomon block at the San Cristobal trench, the northernmost chain is related to southwards-directed subduction of the Pacific Plate beneath the Solomon block at the Vitiaz trench, and the central chain is related to rifting (op. cit.). Kroenke (1995) correlated the Vitiaz volcanic chain with the islands of Anuta and Fatutaka situated further east, south of the Vitiaz trench, which have yielded radiometric ages of ~2 Ma (Jezek et al., 1977). The seafloor imagery data resulting from the Sopacmaps swath mapping project is compelling evidence that subduction has occurred along the Vitiaz trench in very recent geological times, and may be occurring at present. An important conclusion resulting from this assertion is that thinner parts of the OJP potentially may have been subducted *in total* without causing any significant deformation to the Solomon arc.

Yan and Kroenke (1993) suggested that subduction along the SSTS began at around 12 Ma. Within Solomon Islands there is no definitive evidence for subduction-related volcanism until the Upper Miocene: the oldest radiometric date for this volcanic phase is a K–Ar date of 6.4 ± 1.9 Ma for the Gallego volcanics of Guadalcanal (Hackman, 1980). On many islands the oldest volcanism from this period is Pliocene and younger. We suggest that subduction along the SSTS was diachronous (e.g., Mann et al., 1996), with subduction beginning in the east, in the Fiji area, gradually moving westwards and beginning in the Makira–Guadalcanal area at ~8–7 Ma (Fig. 13; Table 1). The intermittent volcanism at this time may be because of an incomplete record

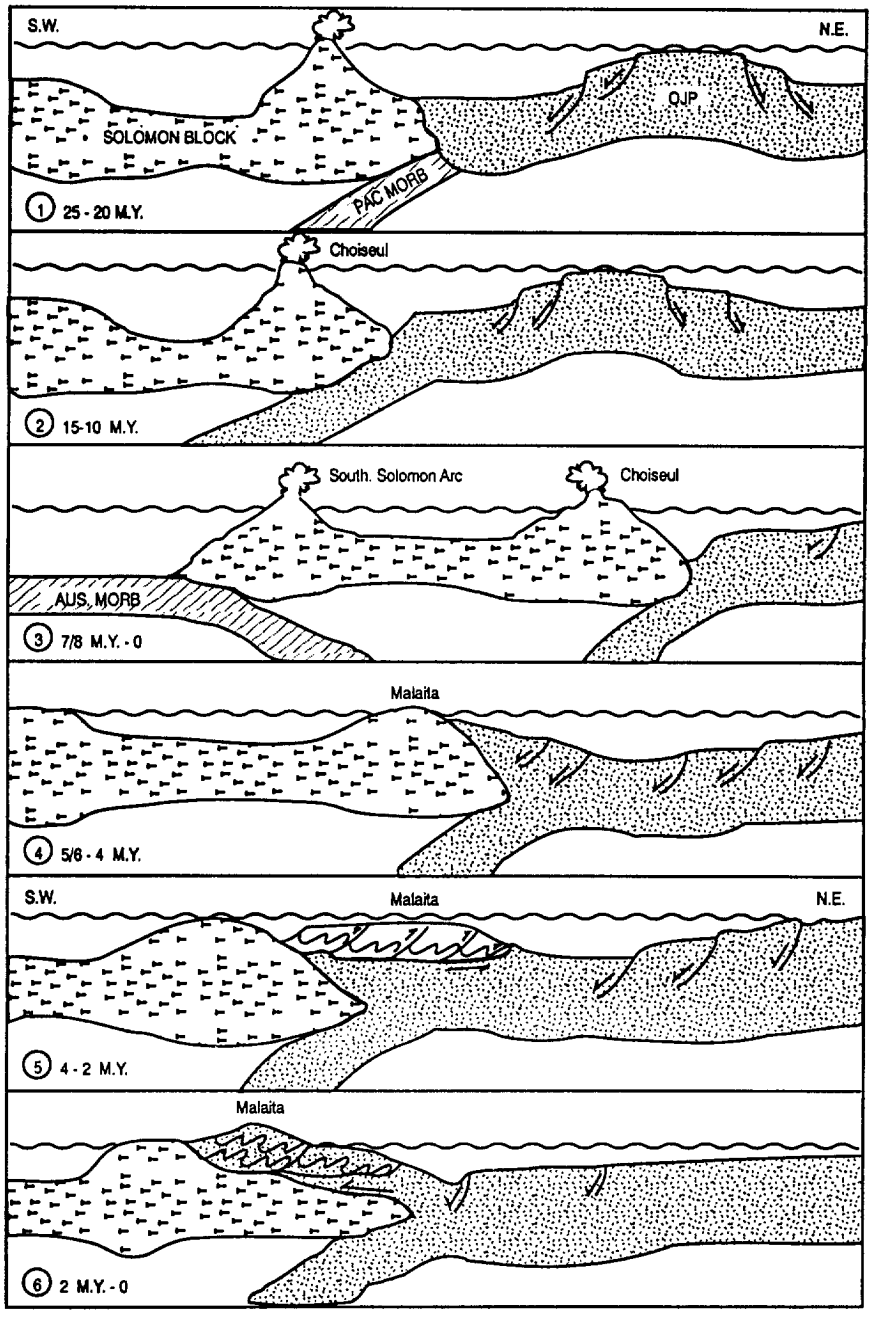

Fig. 13. Cartoon diagram illustrating tectonic model for the OJP–Solomon arc collision. (1) 25–20 Ma. Initial 'soft docking' between the OJP and the Solomon arc. Cessation of SE-directed subduction at Vitiaz trench. (2) 15–10 Ma. Resumption of localised, intermittent, passive subduction of the OJP at the Vitiaz trench. Volcanism on Choiseul and east of Makira. (3) 7/8 Ma–present day. Commencement of main NE-directed subduction at South Solomon trench system. Stage-2 Solomon arc commences. (4) 5/6–4 Ma. Increased coupling between Solomon arc and OJP causes uplift of Malaita from abyssal to shallow-marine depths. (5) 4–2 Ma. Malaita shortened with the production of NW–SE-trending folds and NE-propagating thrusts. Detachments form at ~6–10 km. Simultaneous subduction of deeper level OJP. (6) 2 Ma–present day. Malaita and Malaita anticlinorium obducted southwestwards over the Solomon arc. Continued subduction of deeper level OJP.

or either low-angle subduction and/or the temporary plugging of the trench by thicker portions of the OJP (cf. Cloos, 1993).

5.4. Formation of the Malaita anticlinorium and obduction of Malaita

Increased coupling between the OJP and Solomon block, possibly caused by the entry of the then newly formed and relatively hot Woodlark basin oceanic lithosphere into the SSTS close to present-day Makira, resulted in the formation of the Malaita anticlinorium (which includes the island of Malaita; Kroenke, 1972) (Fig. 2). While deformation present within other parts of the Malaita anticlinorium could have perhaps occurred during the mid-Early Miocene, the first indications of an imminent deformation event in the sedimentary record of Malaita are recorded within the Miocene–Lower Pliocene Suafa Formation. Unlike any of the older sediments of Malaita, the Suafa Formation contains relatively shallow-marine facies with current bedding structures and benthonic fauna. We interpret this change of sedimentary facies as indicating the gradual emergence of Malaita from abyssal depths to much shallower levels; this uplift occurred during Late Miocene/Early Pliocene times (Fig. 13; Table 1).

The age of the main compressive–transpressive deformational event on Malaita island is stratigraphically placed at mid-Pliocene. One of the key conclusions from structural studies of Malaita is that the earliest stage of deformation involved a general movement of material towards the northeast. There are a number of published seismic sections which support the Malaita vergence data, and provide insights into the origin of the NE-moving structures. Kroenke (1972) included several seismic sections which are relevant here. For example, fig. 11 of Kroenke (1972) depicts NE-trending nappe-like structures north of the Cape Johnson trench (at least five discrete nappes are imaged), and fig. 17 (Kroenke, 1972) depicts NE-verging asymmetrical folds northeast of Santa Isabel, with southwesterly dipping, northeast-verging thrusts cutting both cover and basement sequences. P. Mann (pers. commun., 1995), has produced enhanced seismic reflection images from data of Bruns et al. (1986, 1989). One of these images is a NE–SW-oriented section across the Ramos Ridge situated between Santa Isabel and Malaita, and clearly shows NE-verging folds within the sedimentary cover sequence. These seismic images clearly show that structures which are very similar in shape, style, and vergence to those exposed on Malaita are widespread throughout the Malaita anticlinorium.

Some of the NE-vergent thrusts on Malaita may be reactivated normal faults. Kroenke (1972) presented seismic images of the Roncador–Stewart arch area of the OJP, north of Malaita (Fig. 2) which reveal a number of major extensional faults. Furthermore, Coleman and Kroenke (1981) suggested that extensional structures formed within the OJP as a result of the buckling and arching of OJP lithosphere as it approached the Vitiaz subduction zone. Extensional faults would also form within the OJP shortly after the original emplacement event as the plateau cooled and contracted, or as it passed over the Samoan or Raratongan hotspot. Once formed (by whatever method), these extensional faults would become permanent crustal fractures which may be reactivated during a later compressional tectonic regime. Alternatively, the Malaitan thrusts may use natural lithological weakness zones, such as lava–lava contacts or rare sedimentary interbeds, as detachment zones. In essence, our interpretation of the above data is that during the mid-Pliocene (4 Ma to 2 Ma) Malaita (and other OJP-related Solomon Islands such as northern Santa Isabel and Ulawa) was shortened and overthrusted *towards* the northeast (Fig. 13; Table 1).

5.4.1. 2 Ma–present day: detachment and transport of the OJP

Data discussed above suggest that southwards-directed subduction of the OJP along the Vitiaz trench is possibly occurring at the present time and has been doing so since the Late Miocene–Pliocene. This subduction occurred penecontemporaneously with the 5–2 Ma emergence, shortening, and obduction phase of the OJP. The final event in the obduction of the OJP was the detachment of a flake of the OJP upper crust from a horizon at ~5–10 km, and the subsequent southwestwards transport of this flake across the North Solomon trench. Numerous NW–SE submarine ridges in the vicinity of

Malaita have been imaged by the recent Sopacmaps seafloor swath mapping survey (Sopacmaps, 1994; Kroenke, 1995). These ridges have the morphology of SW-verging frontal thrust ramparts and associated foreland basins, with sediment shedding into the foreland basin from the frontal thrust ridge (Kroenke, 1995). These structures may also have an analogue on Malaita as the late SW-directed backthrusts and SW-verging major folds identified in the Kwaio backthrust belt. The SW-verging structures provided a mechanism for the OJP to cross the North Solomon trench and thrust over the Solomon arc.

6. Implication

We stress that the flake tectonic model presented above is only one of a number of possible models which could explain the formation of the Malaita anticlinorium. However, while there are other interpretations to the data, it is our conclusion that they best support the model presented above. This model uses structural data and field observations from Malaita in conjunction with geophysical surveys of the surrounding submerged crust to describe the tectonic history of the OJP from formation to its present-day location at the boundary of the Australian and Pacific plates. The major implication of this model is that it predicts that the southern edge of the OJP in the vicinity of Malaita is essentially split into two components. The Solomon arc block is indenting the OJP in such a way that the upper 5–10 km of the OJP are being detached and overthrusted southwestwards over the Solomon arc block, whilst deeper parts of the OJP edge are being subducted (Fig. 13; Table 1). If this model is correct, it suggests that even the largest and thickest of oceanic plateaus are not necessarily preserved completely intact and are inherently, at least in part, subductable. This may explain the relative lack of obducted plateau remnants in the continental crustal record.

Acknowledgements

This paper is published by permission of the Director of Geology, Ministry of Energy, Water, and Mineral Resources, Honiara, Solomon Islands. We are indebted to the field staff of the above ministry for their invaluable field support; in particular, we thank Peter Diau, Stanley Basi, Henry Mahoa, Andrew Mason, Primo Amusae, Watson Satokana, Lynston Tivuru, Andrew Saelani, and Alan Ramo. We thank all chiefs, landowners, and labourers from Malaita without whom this work would not have been possible. Ed Silver and Zvi Ben-Avraham are thanked for thoughtful and insightful reviews.

References

Allen, J.B., Deans, T., 1965a. An alnöite breccia associated with the ilmenite–pyrope gravels of Malaita, 1962. Rep. 49A, British Solomon Islands Geological Record 2, 1959–1962, pp. 136–138.

Allen, J.B., Deans, T., 1965b. An alnöite breccia and ankaratrite associated with the ilmenite–pyrope gravels of Malaita, 1962. Rep. 49B, British Solomon Islands Geological Record 2, 1959–1962, pp. 138–141.

Allen, J.B., Deans, T., 1965c. Ultrabasic eruptives with alnöitic–kimberlitic affinities from Malaita, Solomon Islands. Mineral. Mag. 34, 16–34.

Allen, J.B., Deans, T., 1968. Ultrabasic eruptives with alnöitic–kimberlitic affinities from Malaita, Solomon Islands. Rep. 76, British Solomon Islands Geological Record 3, 1963–1967, pp. 50–51.

Allum, J.A.E., 1967. Regional photogeological interpretation of the British Solomon Islands. Aerial geophysical surveys project UNSF–BSIP, 1965–1968. Rep. A6, Geology Division, Ministry of Natural Resources, Solomon Islands.

Arthur, M.A., Dean, W.E., Schlanger, S.O., 1985. Variations in the global carbon cycle during the Cretaceous related to climate, volcanism, and changes in atmospheric CO_2. In: Sundquist, E.T., Broecker, W.S. (Eds.), The Carbon Cycle and Atmospheric CO_2: Natural Variations Archean to Present. AGU, Geophys. Monogr. 32, 504–529.

Barron, A.J.M., 1993. The geology of northernmost Malaita. A description of sheets 8/160/7 and 8/160/8. Publication of the Geological Survey Division, Ministry of Natural Resources, Honiara, TR 5/93.

Ben-Avraham, Z., Nur, D., Jones, D., Cox, A., 1981. Continental accretion: from oceanic plateaus to allochthonous terranes. Science 213, 47–54.

Bercovici, D., Mahoney, J.J., 1994. Double flood basalts and plume head separation at the 660 km discontinuity. Science 266, 1367–1369.

Berger, W.H., Kroenke, L.W., Mayer, L.A., Backman, J., Janacek, T.R., Krissek, L., Leckie, M., Lyle, M., 1992. The record of Ontong Java Plateau: main results of ODP Leg 130. Geol. Soc. Am. Bull. 104, 954–972.

Bruns, T.R., Cooper, A.K., Vedder, J.G., 1986. A multi-channel seismic reflection profile across the Solomon Islands Arc. In: Vedder, J.G., Pound, K.S., Boundy, S.Q. (Eds.), Geology and Offshore Resources of Pacific Island Arcs – Central and Western Solomon Islands. Earth Science Series 4, Circum-Pacific Council for Energy and Mineral Resources Houston, TX, pp. 215–224.

Bruns, T.R., Vedder, J.G., Hart, P.E., Mann, D.M., 1989. Multichannel seismic-reflection profiles across the Solomon Islands Arc: Guadalcanal–Malaita, Vella–Lavella–Choiseul, and Bougainville–Buka regions. In: Vedder, J.G., Bruns, T.R. (Eds), Geology and Offshore Resources of Pacific Island Arcs – Solomon Islands and Bougainville – PNG regions. Earth Science Series 12, Circum-Pacific Council for Energy and Mineral Resources Houston, TX, pp. 323–328.

Chivas, A.R., 1981. Geochemical evidence for magmatic fluids in porphyry copper mineralization, Part 1. Mafic silicates from the Koloula Igneous Complex. Contrib. Mineral. Petrol. 78, 389–403.

Cloos, M., 1993. Lithospheric buoyancy and collisional orogenesis: subduction of oceanic plateaus, continental margins, island arcs, spreading ridges, and seamounts. Geol. Soc. Am. Bull. 105, 715–737.

Coleman, P.J., 1965. Stratigraphical and structural notes on the British Solomon Islands with reference to the first geological map, 1962. Rep. 29, British Solomon Islands Geological Record 2, 1959–1962, pp. 17–33.

Coleman, P.J., 1966. The Solomon Islands as an island arc. Nature 211, 1249–1251.

Coleman, P.J., 1970. Geology of the Solomon and New Hebrides Islands, as part of the Melanesian Re-entrant, SW Pacific. Pac. Sci. 24, 289–314.

Coleman, P.J., Kroenke, L.W., 1981. Subduction without volcanism in the Solomon Islands Arc. Geo-Mar. Lett. 1, 129–134.

Cooper, P.A., Taylor, B., 1984. The spatial distribution of earthquakes, focal mechanisms, and subducted lithosphere in the Solomon Islands. In: Exon, N.F., Taylor, B. (Eds.), Marine Geology, Geophysics, and Geochemistry of the Woodlark Basin, Solomon Islands. Earth Science Series 7, Circum-Pacific Council for Energy and Mineral Resources, Houston, TX, pp. 67–88.

Cooper, P.A., Kroenke, L.W., Resig, J.M., 1986. Tectonic implications of seismicity northeast of the Solomon Islands. In: Vedder, J.G., Pound, K.S., Boundy, S.Q. (Eds.) Geology and Offshore Resources of Pacific Island Arcs – Central and Western Solomon Islands. Earth Science Series 4, Circum-Pacific Council for Energy and Mineral Resources, Houston, TX, pp. 117–122.

Coulson, F.I., Vedder, J.G., 1986. Geology of the central and western Solomon Islands. In: Vedder, J.G., Pound, K.S., Boundy, S.Q. (Eds.), Geology and Offshore Resources of Pacific Island Arcs – Central and Western Solomon Islands. Earth Science Series 4, Circum-Pacific Council for Energy and Mineral Resources, Houston, TX, pp. 59–87.

Danitofea, S., 1981. The geology of Ulawa Island, Solomon Islands. Rep. G6, Geology Division, Ministry of Natural Resources, Honiara, 56 pp.

Davis, G.L., 1977. The ages and uranium contents of zircons from kimberlites and associated rocks. Ext. Abstr. 2nd Int. Kimberlite Conference, Santa Fe, NM.

Duncan, R.A., Hargreaves, R.B., 1984. Plate tectonic evolution of the Caribbean region in the mantle reference frame. In: Bonini, W.E., Hargreaves, R.B., Shagam, R. (Eds.), The Caribbean–South America Plate Boundary and Regional Tectonics. Geol. Soc. Am. Mem. 162, 81–93.

Dunkley, P.N., 1983. Volcanism and the evolution of the ensimatic Solomon Islands Arc. In: Shimozuru, D., Yokoyama, I. (Eds.), Arc Volcanism: Physics and Tectonics. Terra, Tokyo, pp. 225–241.

Dunkley, P.N., 1986. Geology of the New Georgia Group, Solomon Islands. British Geological Survey Overseas Directorate: British Technical Cooperation Project, Western Solomon Islands Geological Mapping Project 21; Report MP/86/6, British Geological Survey.

Hackman, B.D., 1968. Observations on folding in the Oligocene–Miocene limestones of central Kwara'ae, Malaita. Rep. 76, British Solomon Islands Geological Record 3, 1963–1967, pp. 47–50.

Hackman, B.D., 1973. The Solomon Islands fractured arc. In: Coleman, P.J. (Ed.), The Western Pacific: Island Arcs, Marginal Seas, Geochemistry. University of Western Australia Press, Perth.

Hackman, B.D., 1980. The geology of Guadalcanal, Solomon Islands. Overseas Mem. Inst. Geol. Sci. 6, 115 pp. + map.

Hawkins, M.P., Barron, A.J.M., 1991. The geology and mineral resources of Santa Isabel, Solomon Islands. Ministry of Natural Resources, Honiara, 114 pp. + maps.

Hine, N., 1991. Calcareous nannofossil study of Upper Cretaceous to Pliocene sediments from Northern Malaita. British Geological Survey Technical Report, Stratigraphic Series, Rep. No. PD/91/278.

Hughes, G.W., Turner, C.C., 1976. Geology of southern Malaita. Solomon Islands Geology Division, Bull. 2. Publication of the Geological Survey Division of the Ministry of Natural Resources, Honiara, 80 pp.

Hughes, G.W., Turner, C.C., 1977. Upraised Pacific ocean floor, southern Malaita, Solomon Islands. Geol. Soc. Am. Bull. 88, 412–424.

Ito, G., Clift, P., 1996. Evidence for multi-staged accretion of the Manihiki and Ontong Java Plateaus from their vertical tectonic histories (abstr.). EOS Trans. Am. Geophys. Union 77, 714.

Jezek, P.A., Bryon, W.B., Haggarty, S.E., Johnson, P., 1977. Petrography, petrology, and tectonic implications of Mitre Island, northern Fijian Plateau. Mar. Geol. 24, 123–148.

Johnson, R.W., Tuni, D., 1987. Kavachi, and active forearc volcano in the Western Solomon Islands. In: Taylor, B., Exon, N.F. (Eds.), Marine Geology, Geophysics, and Geochemistry of the Woodlark Basin – Solomon Islands. Earth Science Series 7, Circum-Pacific Council for Energy and Mineral Resources, Houston, TX, pp. 89–112.

Johnson, R.W., Jaques, A.L., Langmuir, C.H., Perfit, M.R., Staudigel, H., Dunkley, P.N., Chappell, B.W., Taylor, S.R., Baekasapa, M., 1987. Ridge subduction and forearc volcanism: petrology and geochemistry of rocks dredged from the Western Solomon Arc and Woodlark Basin. In: Taylor, B., Exon, N.F. (Eds.), Marine Geology, Geophysics, and Geochemistry of the Woodlark Basin – Solomon Islands. Earth Science Series 7, Circum-Pacific Council for Energy and Mineral Resources, Houston, TX, pp. 155–226.

Kokelaar, B.P., 1982. Fluidisation of wet sediments during the

emplacement and cooling of various igneous bodies. J. Geol. Soc. London 139, 21–33.

Kroenke, L.W., 1972. Geology of the Ontong Java Plateau. Ph.D Thesis, Hawaii Inst. of Geophysics, Univ. of Hawaii, 119 pp. + maps and seismic sections.

Kroenke, L.W., 1984. Cenozoic tectonic development of the southwest Pacific. U.N. ESCAP, CCOP/SOPAC Tech. Bull. 6, pp. 1–22.

Kroenke, L.W., 1995. A morphotectonic interpretation of SOPACMAPS 1 : 500,000 charts. Central Solomon Islands – Southern Tuvalu. Technical Rep. 220, SOPAC, Fiji.

Kroenke, L.W., Resig, J.M., Cooper, P.A., 1986. Tectonics of the southeastern Solomon Islands: Formation of the Malaita anticlinorium. In: Vedder, J.G., Pound, K.S., Boundy, S.Q. (Eds.), Geology and Offshore Resources of Pacific Island Arcs – Central and Western Solomon Islands. Earth Science Series 4, Circum-Pacific Council for Energy and Mineral Resources, Houston, TX, pp. 109–116.

Kroenke, L.W., Berger, W.H., et al., 1991. Proceedings of the Ocean Drilling Program, Initial Results. Ocean Drilling Program 130, 1240 pp.

Kroenke, L.W., Resig, J.M., Leckie, R.M., 1993. Hiatus and tephrachronology of the Ontong Java Plateau: correlation with regional tectono-volcanic events. Proc. ODP, Sci. Results 130, 423–444.

Mahoa, H., Petterson, M.G., 1995. Stream sediment geochemistry of north-central Malaita: implications for mineral reconnaissance and geological studies. Publication of the Water and Mineral Resources Division, Ministry of Energy, Water and Mineral Resources, Honiara, Mem. 2/95.

Mahoney, J.J., 1987. An isotopic survey of Pacific oceanic plateaux: implications for their nature and origin. AGU, Geophys. Monogr. 43, 207–220.

Mahoney, J.J., Storey, M., Duncan, R.A., Spencer, K.J., Pringle, M., 1993a. Geochemistry and geochronology of the Ontong Java Plateau. In: Pringle, M., Sager, W., Sliter, W., Stein, S. (Eds.), The Mesozoic Pacific. AGU, Geophys. Monogr. 77, 233–261.

Mahoney, J.J., Neal, C.R., Petterson, M.G., McGrail, B.A., Saunders, A.D., Babbs, T.L., Norry, M.J., 1993b. Formation of an oceanic plateau: speculations from field and geophysical observations of the Ontong Java Plateau. EOS Trans. Am. Geophys. Union 74, 552.

Mann, P., Gahagan, L., Coffin, M., Shipley, T., Cowley, S., Phinney, E., 1996. Regional tectonic effects resulting from the progressive East-to-West collision of the Ontong Java Plateau with the Melanesian Arc System (abstr.) . EOS Trans. Am. Geophys. Union, Fall Meeting Suppl. 77, 712.

McTavish, R.A., 1966. Planktonic foraminifera from the Malaita Group, British Solomon Islands. Micropalaeontology 12, 1–36.

Neal, C.R., 1985. Mantle Studies in the Western Pacific and Kimberlite-Type Intrusives. Unpubl. Ph.D. Thesis, Univ. of Leeds, 365 pp.

Neal, C.R., 1988. The origin and composition of metasomatic fluids and amphiboles beneath Malaita, Solomon Islands. J. Petrol. 29, 149–175.

Neal, C.R., 1995. The relationship between megacrysts and their host magma and identification of the mantle source region. EOS Trans. Am. Geophys. Union 76, 664.

Neal, C.R., Davidson, J.P., 1989. An unmetasomatised source for the Malaitan alnöite (Solomon Islands): petrogenesis involving zone refining, megacryst fractionation, and assimilation of oceanic lithosphere. Geochim. Cosmochim. Acta 53, 1975–1990.

Neal, C.R., Mahoney, J.J., Kroenke, L.W., Duncan, R.A., Petterson, M.G., 1997. The Ontong Java Plateau. AGU, Geophys. Monogr., in press.

Neef, G., Plimer, I.R., 1979. Ophiolite complexes on Small Ngella Island, Solomon Islands. Bull. Geol. Soc. Am. 90, 313–348.

Nixon, P.H., Coleman, P.J., 1978. Garnet-bearing lherzolites and discrete nodule suites from the Malaita alnöite, Solomon Islands, and their bearing on the nature and origin of the Ontong Java Plateau. Bull. Aust. Soc. Explor. Geophys. 9, 103–106.

Nixon, P.H., Neal, C.R., 1987. Ontong Java Plateau: deep seated xenoliths from thick oceanic lithosphere. In: Nixon, P.H. (Ed.), Mantle Xenoliths. John Wiley, New York, pp. 335–346.

Nixon, P.H., Mitchell, R.H., Rogers, N.W., 1980. Petrogenesis of alnöitic rocks from Malaita, Solomon Islands, Melanesia. Mineral. Mag. 43, 587–596.

Nur, A., Ben-Avraham, Z., 1982. Oceanic plateaus, the fragmentation of continents, and mountain building. J. Geophys. Res. 87, 3644–3661.

Petterson, M.G., 1995. The geology of north and central Malaita, Solomon Islands. (Including implications of geological research on Makira, Savo, Isabel, Guadalcanal, and Choiseul between 1992 and 1995). Geol. Mem. 1/95, Publication of Water and Mineral Resources Division, Honiara.

Petterson, M.G., Neal, C.R., Mahoney, J.J., Saunders, A.D., Babbs, T.L., Duncan, R.A., Tolia, D., Magu, R., Qopoto, C., Mahoa, H., Natogga, D., 1997. Geologic–tectonic framework of Solomon Islands, SW Pacific. Crustal accretion and growth within an intra-oceanic setting. Tectonics, submitted.

Pound, K.S., 1986. Correlation of rock units in the Central and Western Solomon Islands. In: Vedder, J.G., Pound, K.S., Boundy, S.Q. (Eds.), Geology and Offshore Resources of Pacific Island Arcs – Central and Western Solomon Islands. Earth Science Series 4, Circum-Pacific Council for Energy and Mineral Resources Houston, TX, pp. 89–97.

Ramsay, J.G., Huber, M.I., 1987. The Techniques of Modern Structural Geology, Vol. 2. Folds and Fractures. Academic Press, New York, 462 pp.

Richards, J.R., Cooper, J.A., Webb, A.W., Coleman, P.J., 1966. Potassium–argon measurements of the age of the basalt schists in the British Solomon Islands. Nature 211, 1251–1252.

Richards, M.A., Jones, D.L., Duncan, R.A., DePaolo, D.J., 1991. A mantle plume initiation model for the Wrangellia flood basalt and other oceanic plateaus. Science 252, 263–267.

Rickwood, F.K., 1957. Geology of the island of Malaita. Colon. Geol. Miner. Resour. 6, 300–306.

Ridgeway, J., Coulson, F.I.E., 1987. The geology of Choiseul and the Shortland Islands, Solomon Islands. Overseas Mem. 8, British Geological Survey, HMSO, London, 134 pp. + maps.

Saunders, A.D., Babbs, T.L., Norry, M.J., Petterson, M.G., McGrail, B.A., Mahoney, J.J., Neal, C.R., 1993. Depth and emplacement of oceanic plateau basaltic lavas, Ontong Java Plateau and Malaita, Solomon Islands: implications for the formation of oceanic LIP's?. EOS Trans. Am. Geophys. Union 74, 552.

Snelling, N.J., Ingram, I.H., Chan, K.P., 1970. K–Ar determinations on samples from the British Solomon Islands Protectorate. Unit. Rep. Isot. Geol. Geochem. Div. Inst. Geol. Sci., pp. 70–14.

Sopacmaps, 1994. Report Numbers, 192 (Central solomon Trough), 194 (Malaita), and 195 (Melanesian Arc Gap). SOPAC, Suva.

Storey, M., Mahoney, J.J., Kroenke, L.W., Saunders, A.D., 1991. Are oceanic plateaus sites of komatiite formation?. Geology 19, 376–379.

Sun, S.-S., McDonough, W.F., 1989. Chemical and isotopic systematics of oceanic basalts: implications for mantle composition and processes. In: Saunders, A.D., Norry, M.J. (Eds.), Magmatism in the Ocean Basins. Geol. Soc. Spec. Publ. 42, 313–345.

Tejada, M.L.G., Mahoney, J.J., Duncan, R.A., Hawkins, M.P., 1996. Age and geochemistry of basement and alkalic rocks of Malaita and Santa Isabel, southern margin of the Ontong Java Plateau. J. Petrol. 37, 361–394.

Thierstein, H.R., 1979. Paleoceanographic implications of organic carbon and carbonate distribution in Mesozoic deep sea sediments. In: Talwani, M., Hay, W.W., Ryan, W.B.F. (Eds.), Deep Drilling Results in the Atlantic Ocean: Continental Margins and Paleoenvironment. AGU, M. Ewing Ser. 3, 249–274.

Turner, C.C., Ridgeway, J., 1982. Tholeiitic, calc-alkaline, and (?) alkaline igneous rocks of the Shortland Islands, Solomon Islands. In: Packham, G.H. (Ed.), The Evolution of the India–Pacific Plate Boundaries. Tectonophysics 87, 335–354.

Van Deventer, J., Postuma, J.A., 1973. Early Cenomanian to Pliocene deep-marine sediments from North Malaita, Solomon Islands. J. Geol. Soc. Aust. 20, 145–150.

Yan, C.Y., Kroenke, L.W., 1993. A plate tectonic reconstruction of the Southwest Pacific, 0–100 Ma. Proc. ODP Sci. Res. 130, 697–709.